Optimal Positioning of Flying Base Stations and Transmission Power Allocation in NOMA Networks

Mohammadsaleh Nikooroo, *Member, IEEE,* Zdenek Becvar, *Senior Member, IEEE*

***Abstract*—Unmanned aerial vehicles (UAVs) acting as flying base stations (FlyBSs) are considered as an efficient tool to enhance the capacity of future mobile networks and to facilitate the communication in emergency cases. These benefits are, however, conditioned by an efficient control of the FlyBSs and management of radio resources. In this paper, we propose a novel solution jointly selecting the optimal clusters of an arbitrary number of the users served at the same time-frequency resources by means of non-orthogonal multiple access (NOMA), allocating the optimal transmission power to each user, and determining the position of the FlyBS. This joint problem is constrained with the FlyBS's propulsion power consumed for flying and with a continuous guarantee of a minimum required capacity to each mobile user. The goal is to enhance the duration of a communication coverage in NOMA defined as the time interval within which the FlyBS always provides the minimum required capacity to all users. The proposed solution clusters the users and allocates the transmission power of the FlyBS to the users efficiently so that the communication coverage provided by the FlyBSs is extended by 67%–270% comparing to existing solutions while the propulsion power is not increased.**

***Index Terms*—Flying base station, non-orthogonal multiple access, user clustering, transmission power, mobile users, mobile networks, 6G.**

I. Introduction

Unmanned aerial vehicles (UAVs) acting as flying base stations (FlyBSs) provide a promising way to address various concerns and challenges in the future mobile networks. Due to a high mobility, the FlyBSs present exclusive features, such as adaptability to the network topology and to the actual users' requirements, in comparison to conventional static base stations [1]. These advantages make the FlyBSs an efficient solution for multiple practical applications including surveillance and monitoring [2], [3], data traffic management [4], emergency missions [5], network coverage enhancement [6], [7], data gathering from IoT devices [8], or improving users' quality of service [1], [9], [10].

A critical and limiting aspect in the networks with FlyBSs is a power consumption. In [11], an efficient positioning of the FlyBSs is proposed to maximize the number of covered users while reducing the transmission power in orthogonal multiple access (OMA) network. However, the power consumption due to movement of the FlyBS (denoted as propulsion power) is not considered. Furthermore, the problem of a throughput improvement in the OMA-based mobile networks with FlyBSs is addressed in [12]. Then, in [13], the authors maximize the throughput via a positioning of the FlyBS in the mobile networks with OMA. However, neither the transmission nor the propulsion power consumption is considered in [12] and [13]. In [14] and [15], the power consumption of the FlyBS serving moving users is optimized and a joint power control and FlyBS's positioning is provided for the networks with OMA.

Non-orthogonal multiple access (NOMA) is considered as a promising technique in future mobile networks [16]. NOMA provides a high spectral efficiency by including a superposition coding at a transmitter and a successive-interference-cancellation (SIC) decoding at a receiver [17]. Thus, NOMA enables to group users into clusters and serve all users in one cluster at the same time-frequency resources with a separation in a power domain [18]. Consequently, NOMA potentially increases throughput and spectral efficiency comparing to OMA [1], [17], [19], [20].

Key challenges related to NOMA include fairness control [21], [22], throughput improvement [23], resource allocation [24], [25], [26], [27], [28], network coverage [29], and pairing (or clustering) of the users served at the same time-frequency resources [24], [30]. These key challenges are even emphasized and extended when NOMA is integrated to the networks with FlyBSs [16]. For example, the clustering schemes developed for the networks with the static base stations consider instantaneous gains of the users' channels as a criteria to find the users' clustering in [24], [30]. However, such approach is not suitable for the networks with the FlyBS, as the next position of the FlyBS is determined based on the current pairing/clustering, while the selected clustering of the users is based on the current position of the FlyBS. Hence, the solutions designed for the static base stations are not suitable for the FlyBSs.

In [31], the problem of optimizing the FlyBS's altitude, antenna beamwidth, and transmission power allocation is investigated to maximize the sum capacity in a multiuser NOMA network. However, the problem of the user's pairing/clustering is not investigated, as the authors assume the users are already (beforehand) paired into fixed clusters.

Furthermore, in [32], the authors investigate the coverage

Mohammadsaleh Nikooroo and Zdenek Becvar are with Department of Telecommunication Engineering, Faculty of Electrical Engineering, Czech Technical University in Prague, Czech Republic, e-mail: (nikoomoh@fel.cvut.cz, and zdenek.becvar@fel.cvut.cz).

This work has been supported by Grant No. P102-18-27023S funded by Czech Science Foundation and by the grant of Czech Technical University in Prague No. SGS20/169/OHK3/3T/13.

in a network with two static users served by the FlyBS. The authors provide a combination of NOMA and OMA transmission to reduce an outage probability of the users. However, the positioning (trajectory) of the FlyBS is not optimized. Then, in [29], the authors determine the altitude of the FlyBS serving also only two static users in the network with NOMA to maximize Jain's fairness index. The paper [29] is extended in [23] by a power allocation and a determination of the FlyBS's altitude to maximize the sum capacity of two static users. Nevertheless, the x and y coordinates of the FlyBS are fixed. Thus, the flexibility in a spatial deployment offered by the FlyBSs is not fully exploited. In [33], the authors provide a resource allocation for NOMA with the FlyBS to maximize the throughput in a scenario with, again, only two static users. Then, in [34], the authors focus on a problem of the sum capacity maximization via the transmission power allocation and the FlyBS's trajectory optimization in a hybrid network consisting of the FlyBS serving users via OMA and a static base station serving the users via NOMA so that all users served by the static base station are in one cluster. In [35], a joint FlyBS positioning and the transmission power allocation is targeted to improve the sum capacity of the users that are all grouped into just one cluster. Since there is only one cluster of the users considered in [23], [29], [32], [33], [34], [35], the problem of the users' pairing/clustering is not addressed by any of these works.

In [18], a heuristic solution for a joint user clustering and positioning of the FlyBS is proposed to increase the sum capacity. The user clustering for NOMA is limited to only two users (i.e., a pairing of the users) and its generalization to the clustering of more than two users is not straightforward. Moreover, the FlyBS's power consumption is not considered and the provided solution is sub-optimal and loses performance as the number of users increases.

In [36], the authors target to guarantee a secure transmission for static users served by the FlyBS in NOMA considering also a simultaneous wireless information and power transfer (SWIPT). Then, in [37] the authors provide a joint power allocation, beamspace precoding, and FlyBS positioning to maximize an energy efficiency in NOMA with the static users. However, the problem of the propulsion power consumption is addressed in neither [36] nor [37], as the FlyBS is assumed to hover at a fixed position during the entire operation in these papers.

To the best of our knowledge, the transmission power optimization and the optimal clustering of an arbitrary number of users for NOMA in the networks with FlyBSs is not investigated in the literature. However, the problem of the transmission power allocation should not be ignored, as it directly affects the communication coverage in NOMA provided by the FlyBSs. Due to the maximum transmission power limit of any transmitter in real world application, including the FlyBSs, the FlyBS might fail to satisfy the minimum capacity required by the users if the transmission power in NOMA is not managed and allocated to the users properly. The guarantee of the minimum capacity is mandatory in many real-time applications, such as assisted or autonomous driving, or in emergency situations. Many works focus on the transmission power optimization of the FlyBSs for a variety of OMA scenarios, see e.g., [1], [9], [14]. However, in NOMA, the transmission power becomes an even more critical aspect, as adopting an inefficient clustering of the users and power allocation can lead to a requirement on a very high transmission power beyond the maximum allowed transmission power of the FlyBS and to an inability to guarantee the users' required capacity.

In this paper, we propose a joint clustering of the users for NOMA, optimal allocation of the transmission power for NOMA, and optimal FlyBS's positioning to enhance a duration of the communication coverage in NOMA networks. Moreover, we consider practical constraints on the FlyBS's speed, acceleration, and propulsion power consumption, while continuously guaranteeing a minimum communication capacity to each mobile user. The detailed contribution and novelty presented in our paper are as follow:

- We express analytically the transmission power consumption as a function of i) the user clustering for NOMA, ii) the users' minimum required downlink capacity, and iii) the users' relative locations with respect to the FlyBS. Then, the minimum achievable transmission power is expressed in terms of these parameters.
- As a major contribution, we derive a low-complexity analytical solution determining the optimum user clustering for NOMA with an arbitrary number of users in every cluster, and we determine the corresponding position of the FlyBS to optimize the transmission power allocation. This enables to increase the communication coverage provided by the FlyBS while continuously guaranteeing the minimum capacity required by the mobile user.
- We also take the propulsion power consumption into account to make the proposed solution efficient in terms of a total power consumption and we propose a method to control the propulsion power considering the speed and acceleration limits of the FlyBSs.
- By simulations, we show that our proposed clustering of the users for NOMA, transmission power allocation to the users in the same NOMA cluster, and FlyBS's positioning significantly enhances the communication coverage in NOMA provided by the FlyBS and we show that our proposal is applicable also to a scenario with multiple FlyBSs.

Note that this paper is an extension of our prior work [38], where we outline a general idea of the transmission power optimization for the FlyBS with NOMA and we provide initial results.

The rest of the paper is organized as follow. In Section II, we present the system model and formulate the problem of joint NOMA clustering, transmission power allocation, and FlyBS's positioning. The proposed solution is introduced

and thoroughly described in Section III. The performance of the proposed solution and a comparison with state-of-the-art solutions are discussed in Section IV. Last, Section V concludes the paper and outlines future research directions.

II. System Model and Problem Formulation

In this section we first explain the model for the user clustering and SIC decoding in the networks with NOMA and with FlyBS, and we provide details about transmission power modeling. Furthermore, we formulate the problem of user clustering, power allocation, and FlyBS's positioning.

A. System Model

We consider one FlyBS serving N_u mobile users $U = \{u_1, u_2, \ldots, u_{N_u}\}$ in an area as shown in Fig. 1. The users are moving in the same direction similar to, e.g., movement of vehicles on a sub-urban/rural road or a highway. The deployment of the FlyBS is a suitable solution in busy traffic or traffic jam situations to improve the network performance, as the conventional network is usually overloaded by many active users located in a relatively small area with a limited network coverage, (see, e.g., [39], [40]). Without loss of generality, we assume the movement of the users is aligned with the x-axis to simplify the notations and explanation of the idea. All N_u users in the area communicate directly with the FlyBS. The FlyBS and the users use single antenna, since the principle of our proposed solution is independent of the number of antennas. The proposed solution can be easily enhanced towards MIMO, as the interference between different clusters in MIMO is canceled by allocating orthogonal resources to different clusters [41]. After the interference cancellation, our solution can be directly applied to MIMO.

Let $\{X(t), Y(t), H(t)\}$ denote the location of the FlyBS at the time t. We assume that the altitude of the FlyBS is fixed at $H(t) = H$ as in many related works, see e.g., [15], [18], [33], [36]. Note that we adopt this assumption, as the height optimization does not change the principle of the proposed solution, however, it makes the mathematical derivations and explanations clearer and easier to follow. In our model, we consider mobile users and, thus, the coordinates of the users as well as of the FlyBS change over time. As commonly expected in the related works, we assume that the current positions of the users are known to the FlyBS (see, e.g., [18], [23], [42]). However, we assume a realistic case, where the positioning information is inaccurate and contains a positioning error. Thus, the known user's position is given as:

$$\begin{aligned} x^G_{i,j}(t) &= x^{exact,G}_{i,j}(t) + e^x_{i,j}(t), \\ y^G_{i,j}(t) &= y^{exact,G}_{i,j}(t) + e^y_{i,j}(t), \end{aligned} \tag{1}$$

where $x^{exact,G}_{i,j}(t)$ and $y^{exact,G}_{i,j}(t)$ are the exact x and y coordinates of the user $u^G_{i,j}$ at the time t, respectively, and $e^x_{i,j}(t)$ and $e^y_{i,j}(t)$ are the positioning errors in x and y coordinates at the time t, respectively. The FlyBS is able to determine its own position as this information is anyway mandatory for a common flying and navigation of the FlyBSs [33].

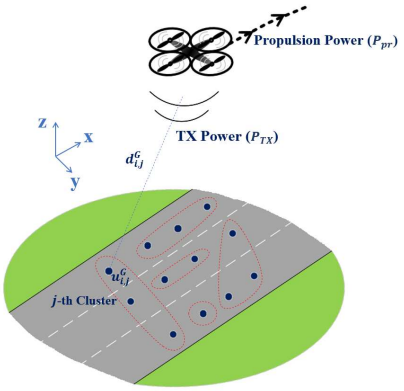

Fig. 1: System model with multiple mobile users (blue dots) deployed within coverage area of the FlyBS and grouped into clusters (red circles) for NOMA purposes.

In NOMA, the users are grouped into clusters such that all users in each cluster share the same frequency at the same time. Thus, the data transmission to the users in the same cluster imposes an interference (referred to as intra-cluster interference). However, there is no interference among different clusters. Let $\mathbb{G}$ denote the space of all possible functions that group the users into N_{cl} clusters such that the number of users in each cluster is larger than or equal to 1 and does not exceed N^{max}_{cu}. For $N_{cl} = 1$, the user in the given cluster is served at orthogonal resources by means of OMA. Furthermore, the maximum cluster size N^{max}_{cu} can be set to an arbitrary value and is practically related to an incurred complexity in SIC decoder. Thus, the maximum cluster size N^{max}_{cu} is typically much lower than the number of users ($N^{max}_{cu} \ll N_u$). Let $N_{cu,j}$ denote the size of the j-th cluster, hence, $N_u = \sum_{j=1}^{N_{cl}} N_{cu,j}$ with $N_{cu,j} \leq N^{max}_{cu}$. Each function $G \in \mathbb{G}$ is defined as a bijective mapping G: $\langle 1, N_u \rangle \rightarrow \langle 1, N_{cl} \rangle \times \langle 1, N^{max}_{cu} \rangle$ and the function G assigns the user u_n as the n_{cu}-th user in the n_{cl}-th cluster if $G(n) = (n_{cl}, n_{cu})$ for the given n. We refer to n_{cu} and n_{cl} as the index of the user in the cluster and the index of the cluster, respectively. Let $u^G_{1,j}, u^G_{2,j}, \ldots, u^G_{N_{cu,j},j}$ denote the users assigned by the clustering function G to the j-th cluster $(1 \leq j \leq N_{cl})$. Then, $\{x^G_{i,j}(t), y^G_{i,j}(t)\}$ represent the coordinates of the user $u^G_{i,j}$ at the time t.

Now we focus on SIC as a common interference cancellation method in NOMA. Suppose that in SIC, the user $u^G_{i,j}$ in the j-th cluster $(1 \leq i \leq N_{cu,j} - 1)$ cancels the interfering signals from the user i' in the same cluster (i.e., $u^G_{i',j}$) for $i + 1 \leq i' \leq N_{cu}$ to extract its own signal. As a result of this, the achievable SINR $\gamma^G_{i,j}, (1 \leq i \leq N_{cu,j})$ for the user $u^G_{i,j}$ is expressed as:

$$\gamma^G_{i,j} = \frac{p^{G,R}_{i,j}(t)}{\sigma^2 + \sum_{l=1}^{i-1} p^{G,R}_{i,l,j}(t)}, (1 \leq i \leq N_{cu,j}), \tag{2}$$

where $p_{i,j}^{G,R}(t)$ represents the received signal power by the user $u_{i,j}^{G}$, $p_{i,l,j}^{G,R}(t)$ denotes the interference power imposed to the user $u_{i,j}^{G}$ by the signal transmitted to the user $u_{l,j}^{G}$ in the same cluster j, and σ^2 is the noise power. Furthermore, let $C_{i,j}^{G}(t)$ denotes the channel capacity of the user $u_{i,j}^{G}$. According to the Shannon–Hartley theorem, the channel capacity $C_{i,j}^{G}(t)$ is defined as:

$$C_{i,j}^{G}(t) = B \times \log_2(1 + \gamma_{i,j}^{G}), \tag{3}$$

where B is the bandwidth assigned to each user and each cluster. As the bandwidth allocation is not a critical aspect for NOMA (it is challenging rather for OMA, see [18], [42]), the channel bandwidth as well as the noise power are assumed to be equal for all clusters.

Now, let us define the model for the transmission power of the FlyBS. The total transmission power of the FlyBS at the time t_k for the user clustering function G is expressed as:

$$P_{TX}(X, Y, H, t_k, G) = \sum_{j=1}^{N_{cl}} \sum_{i=1}^{N_{cu,j}} p_{i,j}^{G,TX}(t_k), \tag{4}$$

where $p_{i,j}^{G,TX}(t_k)$ is the transmission power of the FlyBS to the $u_{i,j}^{G}$. We assume line-of-sight (LoS) communication, since obstacles appear rather exceptionally between the FlyBS at a relatively high altitude and the vehicles on a sub-urban/rural road, hence, the LoS link is dominant. We evaluate LoS probability in our scenario later in Section IV to validate this assumption. According to the Friis' transmission equation, $p_{i,j}^{G,TX}(t_k)$ is determined as:

$$p_{i,j}^{G,TX}(t_k) = \frac{(4\pi f)^{\alpha}}{D_{i,j}^{G,TX} D_{i,j}^{G,R} c^{\alpha}} p_{i,j}^{G,R}(t_k) {d_{i,j}^{G}}^{\alpha}(t_k), \\ (1 \le j \le N_{cl}, 1 \le i \le N_{cu,j}), \tag{5}$$

where α denotes the path-loss exponent, $D_{i,j}^{G,TX}$ is the gain of the FlyBS's antenna, $D_{i,j}^{G,R}$ is the gain of the user's antenna, $d_{i,j}^{G}(t_k)$ represents the distance between the FlyBS and the user $u_{i,j}^{G}$, f is the communication frequency, and $c = 3 \times 10^8$ m/s is the speed of light. The coefficient $\frac{(4\pi f)^{\alpha}}{D_{i,j}^{G,TX} D_{i,j}^{G,R} c^{\alpha}}$ is substituted by Q in the rest of the paper for clarity of the discussions.

Using (5), the total transmission power of the FlyBS is rewritten as:

$$P_{TX}(X, Y, H, t_k, G) = \sum_{j=1}^{N_{cl}} \sum_{i=1}^{N_{cu,j}} Q p_{i,j}^{G,R}(t_k) \times {d_{i,j}^{G}}^{\alpha}(t_k), \tag{6}$$

Furthermore, for the propulsion power, we refer to the model provided in [43] for rotary-wing FlyBSs. In particular, let $V_{FlyBS}(t_k)$ denote the FlyBS's speed at t_k. Then, the propulsion power consumption is expressed as a function of $V_{FlyBS}(t_k)$ as:

$$P_{pr}(t_k) = L_0\big(1 + \frac{3V_{FlyBS}^2(t_k)}{U_{\text{tip}}^2}\big) + \frac{\eta_0 \rho s_r A V_{FlyBS}^3(t_k)}{2} + \\ L_i\Big(\sqrt{1 + \frac{V_{FlyBS}^4(t_k)}{4v_{0,h}^4}} - \frac{V_{FlyBS}^2(t_k)}{2v_{0,h}^2}\Big)^{\frac{1}{2}}, \tag{7}$$

where L_0 and L_i are the blade profile and induced powers in hovering status, respectively, U_{tip} is the tip speed of the rotor blade, $v_{0,h}$ is the mean rotor induced velocity during hovering, η_0 is the fuselage drag ratio, ρ is the air density, s_r is the rotor solidity, and A is the rotor disc area. Interested readers can find more details about the model in [43].

B. Problem Formulation

Our goal is to find the position of the FlyBS jointly with the clustering of the users for NOMA and allocation of the transmission power within NOMA clusters to enhance the duration of the communication coverage (denoted by $T_{coverage}$). The communication coverage is defined as the maximum time step t_k at which i) the FlyBS's battery is yet not fully depleted, and ii) the required transmission power at every time step $t_s \le t_k$ remains below the maximum transmission power limit P_{TX}^{max}. The coverage duration depends on the transmission and propulsion power and, hence, on the FlyBS's position, the NOMA user clustering, and the transmission power allocation to the users in the NOMA clusters. Thus, to maximize $T_{coverage}$, we formulate the joint problem of the user clustering, the transmission power allocation, and the FlyBS's positioning while guaranteeing a minimum capacity for the users during the whole $T_{coverage}$ as follows:

$$\big[G_{opt}, [X_{opt}(t_k), Y_{opt}(t_k)], p_{i,j,opt}^{G_{opt},TX}\big] = \\ \underset{\left[G,[X(t_k),Y(t_k)],p_{i,j}^{G,TX}\right]}{\text{argmax}} \; T_{coverage}, \forall j \in \langle 1, N_{cl} \rangle, \forall i \in \langle 1, N_{cu,j} \rangle, \forall k, \\ s.t. \quad C_{i,j}^{G}(t_k) \ge C_{min}, \forall j \in \langle 1, N_{cl} \rangle, \forall i \in \langle 1, N_{cu,j} \rangle, \forall k, \quad (a) \\ P_{TX}(X, Y, H, t_k, G) \le P_{TX}^{max}, \forall k, \quad (b) \\ \sum_{t_k \le T_{coverage}} (P_{TX}(X, Y, H, t_k, G) + P_{pr}(t_k))(t_k - t_{k-1}) \le E_b. \quad (c) \\ \|\boldsymbol{V}_{FlyBS}(t_k)\| \le V_{FlyBS}^{max}, \quad \forall k, \quad (d) \\ \|\boldsymbol{a}_{FlyBS}(t_k)\| \le a_{FlyBS}^{max}, \quad \forall k. \quad (e) \tag{8}$$

where C_{min} is the minimum instantaneous capacity required by the users, $\|.\|$ denotes the norm of a vector, E_b is the initial available energy in the FlyBS's battery, V_{FlyBS}^{max} and a_{FlyBS}^{max} are the FlyBS's maximum speed and acceleration, respectively, and $\boldsymbol{V}_{FlyBS}(t_k) = \big(V_{FlyBS}^{x}(t_k), V_{FlyBS}^{y}(t_k)\big)$ and $\boldsymbol{a}_{FlyBS}(t_k) = \big(a_{FlyBS}^{x}(t_k), a_{FlyBS}^{y}(t_k)\big)$ are the FlyBS's velocity and acceleration vectors at the time t_k, respectively. The velocity and acceleration vectors are defined, respectively, as:

$$\boldsymbol{V}_{FlyBS}(t_k) = \frac{\big(X(t_k), Y(t_k)\big) - \big(X(t_{k-1}), Y(t_{k-1})\big)}{(t_k - t_{k-1})},$$
$$\boldsymbol{a}_{FlyBS}(t_k) = \frac{\boldsymbol{V}(t_k) - \boldsymbol{V}(t_{k-1})}{(t_k - t_{k-1})}. \quad (9)$$

The constraint (a) in (8) guarantees that every user receives at least the minimum required capacity C_{min} all the time. In line with [18], [24], [33], the minimum capacity is assumed to be the same for all the users. Such assumption corresponds to the case when the minimum required capacity is provided to all users for their essential and critical services, e.g., to a navigation information for the vehicles or to provide/collect control information related to driving. The constraint (b) ensures that the transmission power does not exceed the maximum transmission power limit. Furthermore, the constraint (c) guarantees that the FlyBS's total power consumption does not exceed the maximum capacity of the FlyBS's battery. Furthermore, the constraints (d) and (e) limit the FlyBS's movement in terms of the incurred speed and acceleration, respectively. We propose to extend $T_{coverage}$ via an efficient positioning of the FlyBS considering the transmission power and propulsion power consumption. However, despite the fact that the propulsion power is significantly larger than the transmission power in general, targeting the optimization of the propulsion power at every time step is not an efficient solution, as such approach is not deterministic. In particular, for the propulsion power to be optimal at every time step, it would be sufficient to determine only the FlyBS's speed corresponding to the minimum propulsion power. From the propulsion-power-minimization standpoint, any positioning of the FlyBS that incurs the minimum propulsion power can be regarded as the optimum position of the FlyBS. In such sense, there are potentially infinite candidate positions. However, since the location of the moving users in the next time step(s) is unknown in general, it would not be possible to tell which of the obtained candidate positions would yield the longest coverage duration. In fact, any of those candidate options can be the solution, because the minimum propulsion power is yielded by a movement to any of the candidate positions. Thus, a random selection of the FlyBS's position out of many candidates should be done at every time step.

In contrast, the minimization of the transmission power at every time step with the constrained propulsion power consumption is an efficient strategy. The rationality of this strategy is justified by stressing the fact that the suboptimal transmission power incurs even a larger transmission power (comparing to the transmission power minimization approach) and, thus, the transmission power reaches the maximum limit P_{TX}^{max} faster. Consequently, to extend the duration of the coverage duration in NOMA, the transmission power to users should be allocated so that the total transmission power remains below the maximum limit of P_{TX}^{max}. Such a solution can be provided based a minimization of the transmission power from the early time steps to avoid an increase in the distance between the FlyBS and the optimum position over time. If the distance between the FlyBS and the optimum position would become too large, reaching the optimum position at later time steps might not be possible due to the practical limitations on the FlyBS's speed and acceleration. In contrast, the positioning of the FlyBS to minimize the transmission power at every time step from the beginning keeps the FlyBS constantly close to the position minimizing the transmission power for NOMA, because the FlyBS's optimum positions from one time step to the next time step are typically close to each other.

Hence, we reformulate the problem of $T_{coverage}$ maximization in (8) to the problem of transmission power minimization with a constraint on the propulsion power consumption included so as to address the FlyBS's battery constraint (i.e., constraint (c) in (8)) as follows:

$$\begin{aligned}
&\big[G_{opt}, [X_{opt}(t_k), Y_{opt}(t_k)], p_{i,j,opt}^{G_{opt},TX}\big] = \\
&\underset{\big[G,[X(t_k),Y(t_k)],p_{i,j}^{G,TX}\big]}{\text{argmin}} \quad P_{TX}, \forall j \in \langle 1, N_{cl}\rangle, \forall i \in \langle 1, N_{cu,j}\rangle, \forall k, \\
&s.t. \quad C_{i,j}^{G}(t_k) \geq C_{min}, \forall j \in \langle 1, N_{cl}\rangle, \forall i \in \langle 1, N_{cu,j}\rangle, \forall k, \quad (a) \\
&\qquad P_{TX}(X, Y, H, t_k, G) \leq P_{TX}^{max}, \forall k, \quad (b) \\
&\qquad P_{pr}(t_k) \leq P_{pr,th}(t_k), \quad \forall k, \quad (c) \\
&\qquad \|\boldsymbol{V}_{FlyBS}(t_k)\| \leq V_{FlyBS}^{max}, \quad \forall k, \quad (d) \\
&\qquad \|\boldsymbol{a}_{FlyBS}(t_k)\| \leq a_{FlyBS}^{max}, \quad \forall k, \quad (e)
\end{aligned} \quad (10)$$

where $P_{pr,th}(t_k)$ in the constraint (c) is the upper bound for the propulsion power consumption. The parameter $P_{pr,th}$ establishes a trade-off between the transmission and propulsion power consumption, so that choosing a lower value of $P_{pr,th}$ leads to a reduction in the propulsion power (hence, to a slower depletion of the FlyBS's battery) while it causes an increase in the transmission power, because the FlyBS would have a limited range of speeds during the flight to reach the position minimizing the transmission power. Furthermore, in an extreme case with $P_{pr,th}$ set to the value corresponding to the minimum propulsion power, the problem (10) corresponds to the case when both the propulsion and transmission powers are minimized. In the subsection III.C, we elaborate a setting of $P_{pr,th}$ to tackle the constraint on the capacity of the FlyBS's battery (i.e., constraint (c) in (8)).

III. Proposed optimal clustering of users for NOMA and positioning of FlyBS

In this section, we present a novel solution to the problem defined in (10) by finding the optimal clustering function G_{opt} as well as the optimal FlyBS's positions over time.

Solving the problem of user clustering for NOMA jointly with the FlyBS's positioning in (10) is challenging, as the constraints (c), (d), and (e) define a non-convex region for the FlyBS's position. Furthermore, the set of the clustering options is potentially of a very large size (exponential with the number of users and the NOMA cluster sizes). In addition, the discrete nature of the set of the clustering options for NOMA makes the optimization problem intractable. To deal with these

challenges, we first target the positioning of the FlyBS for arbitrary clustering function G. We solve the problem of positioning by first relaxing the constraints (c), (d), and (e) in (10) (as explained in subsection III.A), and then deriving the solution to the unrelaxed problem (as presented in subsection III.B). Next, we discuss the setting of the parameter $P_{pr,th}$ for the proposed positioning of the FlyBS in subsection III.C. Last, in subsection III.D we discuss how to find the optimal clustering in (10) via a derivation of necessary conditions for the clustering to be optimal. Such necessary conditions help to reduce significantly the size of the set of the clustering options. Now, to solve the problem of the FlyBS's positioning for the clustering function G we lift the constraints (c), (d), and (e), and solve the relaxed problem in terms of the clustering function G. Then, the derived solution is adjusted to fulfill all constraints.

A. Transmission power minimization and FlyBS positioning

In this subsection we focus on the transmission power optimization and the FlyBS's positioning for any NOMA user clustering G, and we derive the FlyBS's position and the transmission power as functions of the clustering. The relaxed problem of the FlyBS's positioning is defined as:

$$\begin{aligned}\left[[X_{opt}(G,t_k),Y_{opt}(G,t_k)],p_{i,j,opt}^{G,TX}\right] = \\ \underset{\left[[X(G,t_k),Y(G,t_k)],p_{i,j}^{G,TX}\right]}{\operatorname{argmin}} P_{TX}, \\ \forall j \in \langle 1, N_{cl}\rangle, \forall i \in \langle 1, N_{cu,j}\rangle, \forall k, \\ s.t. \quad C_{i,j}^{G}(t_k) \geq C_{min}, \forall j \in \langle 1, N_{cl}\rangle, \forall i \in \langle 1, N_{cu}^{max}\rangle, \forall k.\end{aligned} \tag{11}$$

In the following, we solve (11) via a determination of the FlyBS's positioning and the user's power allocation for the NOMA user clustering G. To this end, from the constraint in (11) and using (3), it is inferred that $\gamma_{min} \leq \gamma_{i,j}^{G}$, where $\gamma_{min} = (2^{C_{min}/B} - 1)$ is a positive constant. To find the conditions to reach the minimum transmission power we rewrite $\gamma_{min} \leq \gamma_{i,j}^{G}$ using (2) and (5) as follows

$$\begin{aligned}\gamma_{min}(\sigma^2 + \frac{\sum_{l=1}^{i-1} p_{l,j}^{G,TX}(t_k)}{Q{d_{i,j}^{G}}^{\alpha}(t_k)}) \leq \frac{p_{i,j}^{G,TX}(t_k)}{Q{d_{i,j}^{G}}^{\alpha}(t_k)}, \\ (j \in \langle 1, N_{cl}\rangle, i \in \langle 1, N_{cu,j}\rangle).\end{aligned} \tag{12}$$

After several simple math operations, (12) is transformed to:

$$\begin{aligned}\gamma_{min}\sum_{l=1}^{i-1} p_{l,j}^{G,TX}(t_k) + \gamma_{min}\sigma^2 Q{d_{i,j}^{G}}^{\alpha}(t_k) \leq p_{i,j}^{G,TX}(t_k), \\ (j \in \langle 1, N_{cl}\rangle, i \in \langle 1, N_{cu,j}\rangle).\end{aligned} \tag{13}$$

Therefore, by writing down (13) for every $j \in \langle 1, N_{cl}\rangle$ and $i \in \langle 1, N_{cu,j}\rangle$, we get:

$$\begin{aligned}\sum_{j=1}^{N_{cl}}\sum_{i=1}^{N_{cu,j}} p_{i,j}^{G,TX}(t_k) \geq \\ \gamma_{min}Q\sigma^2\sum_{j=1}^{N_{cl}}\sum_{i=1}^{N_{cu,j}}\left((1+\gamma_{min})^{N_{cu,j}-i}\right){d_{i,j}^{G}}^{\alpha}(t_k).\end{aligned} \tag{14}$$

The minimum in (14) is achieved when the equality in (13) holds for $1 \leq j \leq N_{cl}$ and $1 \leq i \leq N_{cu,j}$. Hence, we derive $P_{TX}(X, Y, H, t_k, G)$ as:

$$\begin{aligned}P_{TX}(X,Y,H,t_k,G) = \\ \gamma_{min}Q\sigma^2\sum_{j=1}^{N_{cl}}\sum_{i=1}^{N_{cu,j}}\left((1+\gamma_{min})^{N_{cu,j}-i}\right){d_{i,j}^{G}}^{\alpha}(t_k)\end{aligned} \tag{15}$$

To find the FlyBS's optimum position (X_{opt}^{G} and Y_{opt}^{G}) and to minimize the transmission power in (15), we exploit Downhill Simplex Algorithm (also known as Nelder-Mead Algorithm). The solution is based on a direct search in two-dimensions and a function comparison using simplex, which is a polytope of $m+1$ vertices among m dimensions. The simplex is updated based on the values obtained from expansion, contraction, and shrinkage operations on the vertex at which the function reaches the largest value, and the centroid of the remaining vertices. Now, we explain the details of the Nelder-Mead Algorithm in our problem (see Algorithm 1). The simplex finds the optimal position of the FlyBS at every time step t_k. For our setup, there is a 2-dimensional point in simplex, with the first and second dimensions corresponding to $X(t_k)$ and $Y(t_k)$, respectively. The values for the three vertices of the simplex (denoted as S_1, S_2, S_3) are determined as follows. First, an initial value for S_3 is guessed (in other

Algorithm 1 Find optimal position of the FlyBS for arbitrary clustering G

$\lambda(A)$: standard deviation of elements in set A, λ_0: standard deviation threshold for termination
$f(S_i)$: Transmission power at t_k evaluated at S_i (i.e., $P_{TX}(S_{i,1}, S_{i,2}, H, t_k, G)$).
Sort and rearrange the points as $f(S_1) \leq f(S_2) \leq f(S_3)$.

while $\lambda(f(S_1), f(S_2), f(S_3))) > \lambda_0$ **do**
  compute $S_0 = \text{centroid}\{S_1, S_2\}$
  if $f(S_1) \leq f(S_r) \leq f(S_2)$ **then** $S_3 \leftarrow S_r$
  else compute $S_e = S_0 + \beta(S_r - S_0)$
  end if
  if $f(S_e) \leq f(S_r)$ **then** $S_3 \leftarrow S_e$, and go to step 13
  else $S_3 \leftarrow S_r$, and go to step 13
  end if
  compute $S_c = S_0 + \nu(S_3 - S_0)$.
  if $f(S_c) \leq f(S_3)$ **then** $S_3 \leftarrow S_c$, and go to step 13
  else compute $S_i = S_1 + \delta(S_i - S_1)$ for $1 \leq i \leq 3$, and go to step 13
  end if
  Sort points so that $f(S_1) \leq f(S_2) \leq f(S_3)$.
end while
From (15) calculate transmission power at S_3

Output: $S_3 = (X_{opt}^{G}(t_k), Y_{opt}^{G}(t_k)) = \text{argmin}_{\{X(t_k),Y(t_k)\}} P_{TX}$, and $P_{TX}^{min}(G, t_k), \forall k$

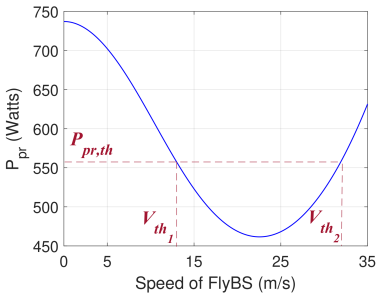

Fig. 2: FlyBS's propulsion power consumption vs. speed. Threshold $P_{pr,th}$ limits the propulsion power consumption and specifies the allowed flight speed range of $[V_{th_1}, V_{th_2}]$.

words, an initial position of the FlyBS at t_k is guessed). We initialize S_3 by the FlyBS's position at the previous time step t_{k-1}. Then, the values for S_1 and S_2 are found by changing the value at one dimension of S_3. In particular, S_3 is initiated with $S_3 = \big(X(t_{k-1}), Y(t_{k-1})\big)$ and, then, S_1 and S_2 are derived as:

$$S_i = \begin{cases} S_3 + \kappa_i S_{3,i} e_i & S_{3,i} \neq 0, \\ S_3 + \epsilon_i e_i & \text{otherwise}, \end{cases} \tag{16}$$

for $1 \leq i \leq 2$, where $S_{3,r}$ denotes the r-th element of S_3, and e_i is the 2-dimensional unit vector with zero elements at all dimensions except the i-th dimension. Furthermore, ϵ_i and κ_i are real coefficients that adjust the convergence of the algorithm. Therefore, the initial simplex includes three different instances of the FlyBS's positions. The algorithm keeps updating the values of the vertices based on expansion, contraction, and shrinkage operations (demonstrated in the lines 4, 9, and 11 in Algorithm 1, respectively) until the standard deviation of the corresponding values of $P_{TX}(X, Y, H, t_k)$ at the simplex's vertices fall below a given threshold.

B. FlyBS's positioning with constrained propulsion power, speed, and acceleration

In the previous subsection, the solution to the FlyBS's position $(X^G_{opt}(t_k), Y^G_{opt}(t_k))$ is derived (in Algorithm 1) to minimize the transmission power for the relaxed optimization problem (11). However, the calculated optimal position $(X^G_{opt}(t_k), Y^G_{opt}(t_k))$ might not be reached at some time steps due to the constraints on the FlyBS's propulsion power, speed, and acceleration, i.e., $P_{pr,th}$, V^{max}_{FlyBS}, a^{max}_{FlyBS}, respectively, in (10). Thus, in this subsection, we address the problem of FlyBS's positioning considering the constraints for the propulsion power, acceleration, and speed. In case the required speed or acceleration to move the FlyBS to the optimal position $(X^G_{opt}(t_k), Y^G_{opt}(t_k))$ (derived from Algorithm 1) exceeds the corresponding limits on the speed or the acceleration (i.e., V^{max}_{FlyBS} and a^{max}_{FlyBS}, respectively), or causes the propulsion power larger than $P_{pr,th}$, the FlyBS moves only to the point that is the closest to the optimal position and, at the same time, can be reached with the speed and the acceleration within their allowed ranges. To derive the point to which the FlyBS should move, let $\big(X^G_{cto}(t_k), Y^G_{cto}(t_k)\big)$ denote the closest point to the optimal position $\big(X^G_{opt}(t_k), Y^G_{opt}(t_k)\big)$ such that the movement from the FlyBS's position at t_{k-1} to $\big(X^G_{cto}(t_k), Y^G_{cto}(t_k)\big)$ does not incur the propulsion power larger than the threshold $P_{pr,th}$ and also the speed and the acceleration are not larger than V^{max}_{FlyBS} and a^{max}_{FlyBS}, respectively. Hence, the problem of FlyBS's positioning is formulated as follows:

$$\begin{aligned} &[\boldsymbol{V}_{FlyBS}(t_k), \boldsymbol{a}_{FlyBS}(t_k), (X^G_{cto}(t_k), Y^G_{cto}(t_k))] = \\ &\underset{\boldsymbol{V}_{FlyBS}(t_k), \boldsymbol{a}_{FlyBS}(t_k)}{\text{argmin}} \; ||(X(t_k), Y(t_k) - (X^G_{opt}(t_k), Y^G_{opt}(t_k))|| \\ &s.t. \quad P_{pr}(t_k) \leq P_{pr,th}(t_k), \quad \forall k \quad (a) \\ &||\boldsymbol{V}_{FlyBS}(t_k)|| \leq V^{max}_{FlyBS}, \quad \forall k \quad (b) \\ &||\boldsymbol{a}_{FlyBS}(t_k)|| \leq a^{max}_{FlyBS}. \forall k \quad (c) \end{aligned} \tag{17}$$

Fig. 2 shows an example of $P_{pr,th}$ and the corresponding range of the FlyBS's speeds $[V_{th_1}, V_{th_2}]$ for which $P_{pr} \leq P_{pr,th}$ for the propulsion power model in (7). The FlyBS's speed should not exceed the allowed range of $[V_{th_1}, \min\{V_{th_2}, V^{max}_{FlyBS}\}]$. Hence, the optimization problem (17) is rewritten by merging the constraints (a) and (b) as a modified constraint on the speed as follows:

$$\begin{aligned} &\big[\boldsymbol{V}_{FlyBS}(t_k), \boldsymbol{a}_{FlyBS}(t_k), \big(X^G_{cto}(t_k), Y^G_{cto}(t_k)\big)\big] = \\ &\underset{\boldsymbol{V}_{FlyBS}(t_k), \boldsymbol{a}_{FlyBS}(t_k)}{\text{argmin}} \; \big\|\big(X(t_k), Y(t_k)\big) - \big(X^G_{opt}(t_k), Y^G_{opt}(t_k)\big)\big\| \\ &s.t. \quad V_{th_1} \leq \|\boldsymbol{V}_{FlyBS}(t_k)\| \leq \min\{V^{max}_{FlyBS}, V_{th_2}\}, \quad (a) \\ &\|\boldsymbol{a}_{FlyBS}(t_k)\| \leq a^{max}_{FlyBS}. \quad (b) \end{aligned} \tag{18}$$

To solve (18), we assume a constant acceleration over very small time steps t_k of the FlyBS's movement. Hence, $\big(X(t_k), Y(t_k)\big)$ is calculated using the motion equation for constant acceleration:

$$\begin{aligned} X(t_k) &= \frac{1}{2}\big(a^x_{FlyBS}(t_k)\big) \times (t_k - t_{k-1})^2 + \\ &\big(V^x_{FlyBS}(t_{k-1})\big) \times (t_k - t_{k-1}) + X(t_{k-1}), \\ Y(t_k) &= \frac{1}{2}\big(a^y_{FlyBS}(t_k)\big) \times (t_k - t_{k-1})^2 + \\ &\big(V^y_{FlyBS}(t_{k-1})\big) \times (t_k - t_{k-1}) + Y(t_{k-1}). \end{aligned} \tag{19}$$

Before presenting the solution to (18), we further elaborate the constraints in (18). Using (19), the constraint (a) in (18) is rewritten as:

$$\begin{aligned} &V_{th_1} \leq \\ &\Big(\big(a^x_{FlyBS}(t_k) + \frac{V^x_{FlyBS}(t_{k-1})}{(t_k - t_{k-1})}\big)^2 + \big(a^y_{FlyBS}(t_k) + \frac{V^y_{FlyBS}(t_{k-1})}{(t_k - t_{k-1})}\big)^2\Big)^{\frac{1}{2}} \\ &\leq \min\{V^{max}_{FlyBS}, V_{th_2}\}. \end{aligned} \tag{20}$$

Furthermore, using the identity $\|\boldsymbol{a}_{FlyBS}(t_k)\| = \big({a^x_{FlyBS}}^2(t_k) + {a^y_{FlyBS}}^2(t_k)\big)^{\frac{1}{2}}$, the constraint (b) in (18) is rewritten in terms of a^x_{FlyBS} and a^y_{FlyBS} as:

$$\big({a^x_{FlyBS}}^2(t_k) + {a^y_{FlyBS}}^2(t_k)\big)^{\frac{1}{2}} \leq a^{max}_{FlyBS}. \tag{21}$$

According to the inequalities in (20), $(a^x_{FlyBS}, a^y_{FlyBS})$ lies inside a ring centered at $\big(-\frac{V^x_{FlyBS}(t_{k-1})}{(t_k-t_{k-1})}, -\frac{V^y_{FlyBS}(t_{k-1})}{(t_k-t_{k-1})}\big)$ with inner and outer radii corresponding to the minimum and maximum limits of $\frac{V_{th_1}}{(t_k-t_{k-1})}$ and $\frac{\min\{V^{max}_{FlyBS}, V_{th_2}\}}{(t_k-t_{k-1})}$, respectively. Fig. 3 shows the region defined by (20) in the $a^x_{FlyBS}-a^y_{FlyBS}$ plane (blue ring). Furthermore, the constraint in (21) defines the inner part of the circle centered at $(0,0)$ with a radius of the FlyBS's acceleration limit a^{max}_{FlyBS} (green circle in Fig. 3). Thus, by incorporating the two constraints in (20) and (21), the problem in (18) is understood as the minimization of $\|\big(X(t_k), Y(t_k)\big) - \big(X^G_{opt}(t_k), Y^G_{opt}(t_k)\big)\|$ over the region enclosed by four curves AB, BC, CD, and DA as shown in Fig. 3.

To proceed with the solution, we use (19) to express the objective function in (18) in terms of $a^x_{FlyBS}(t_k)$ and $a^y_{FlyBS}(t_k)$ as follows:

$$\|\big(X(t_k), Y(t_k)\big) - \big(X^G_{opt}(t_k), Y^G_{opt}(t_k)\big)\| = m\Big(\big(a^x_{FlyBS}(t_k)-\rho_0\big)^2 + \big(a^y_{FlyBS}(t_k)-\sigma_0\big)^2\Big)^{\frac{1}{2}}, \quad (22)$$

$$m = \frac{(t_k - t_{k-1})^2}{2},$$

$$\rho_0 = \frac{\big(V^x_{FlyBS}(t_{k-1})\big)\times(t_k-t_{k-1}) + X(t_{k-1}) - X_{opt}(t_k)}{m},$$

$$\sigma_0 = \frac{\big(V^y_{FlyBS}(t_{k-1})\big)\times(t_k-t_{k-1}) + Y(t_{k-1}) - Y_{opt}(t_k)}{m}.$$

According to (22), the minimum value of $\|\big(X(t_k), Y(t_k)\big) - \big(X^G_{opt}(t_k), Y^G_{opt}(t_k)\big)\|$ is achieved by the closest point $(a^x_{FlyBS}(t_k), a^y_{FlyBS}(t_k))$ to (ρ_0, σ_0). Therefore, the solution to (18) is derived by finding the closest point in the region enclosed by $ABCD$ to (ρ_0, σ_0). To this end, we first find the point on each of the curves AB, BC, CD, and DA that is the closest to (ρ_0, σ_0). Since all the curves AB, BC, CD, and DA are on circles, the closest point to (ρ_0, σ_0) for each curve can be found by finding the intersection of that curve and the line connecting (ρ_0, σ_0) to the center of the circle that the curve lies on. In case that the intersection point lies beyond the curve's endpoints, one of the endpoints yields the minimum distance to (ρ_0, σ_0). The objective function in (22) is evaluated at all four closest candidate points to find the optimal $\big(a^x_{FlyBS}(t_k), a^y_{FlyBS}(t_k)\big)$. Then, we calculate $\big(X(t_k), Y(t_k)\big)$ from (19), which is the optimal solution to (18) (i.e., $\big(X^G_{cto}(t_k), Y^G_{cto}(t_k)\big)$).

C. Determination of $P_{pr,th}$

In this subsection we discuss selection of proper values for the propulsion power limit $P_{pr,th}$ at every time step. Although the proposed solution to the FlyBS's positioning in subsection III.B is valid for any value of $P_{pr,th}$, a fixed $P_{pr,th}$ in (10) may not be very efficient in extending the coverage duration, as the impact of the transmission and propulsion power consumption changes over time due the actual values

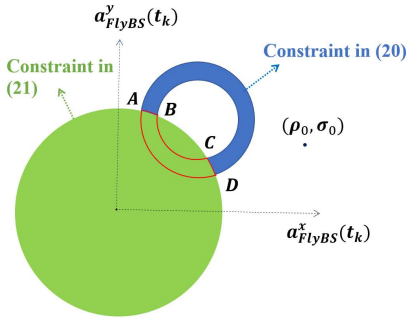

Fig. 3: Regions in $a^x_{FlyBS} - a^y_{FlyBS}$ plane corresponding to the constraints (20) and (21)

of the transmission power and the remaining energy of the FlyBS's battery. Hence, we introduce a varying $P_{pr,th}$ over time. At the beginning, because of a large amount of the remaining energy in the battery, we set $P_{pr,th}$ to the FlyBS's propulsion power consumed at the FlyBS's maximum speed. Then, at every time step t_k ($k > 1$), we estimate the shortest time that it takes for the transmission power to reach the maximum limit of P^{max}_{TX}. More specifically, the estimated time to reach P^{max}_{TX} is denoted by T^{max}_{TX} and calculated as $T^{max}_{TX} = \frac{P^{max}_{TX} - P_{TX}(t_k)}{R^{max}_{TX}(t_k)}$, where $R^{max}_{TX}(t_k)$ is the maximum slope of the increase that can occur between t_k and t_{k+1}. Note that, an accurate evaluation of $R^{max}_{TX}(t_k)$ is not possible in general, as $R^{max}_{TX}(t_k)$ depends on the future location of the users at t_{k+1}. Nevertheless, the values for the slope of the increase in the FlyBS's transmission power in the previous time steps is still a sufficient indicator to estimate $R^{max}_{TX}(t_k)$. Thus, we choose $R^{max}_{TX}(t_k)$ to be the maximum rate of the increase in the transmission power that has actually occurred between two consecutive time steps during the past Δ_t time steps:

$$R^{max}_{TX}(t_k) = \max_s \frac{(P_{TX}(t_s) - P_{TX}(t_{s-1}))}{(t_s - t_{s-1})}, \quad k - \Delta_t + 1 \le s \le k. \quad (23)$$

Choosing lower values for Δ_t results in a less accurate estimation of R^{max}_{TX}, but also an adoption of too high values for Δ_t may result in an inaccurate estimation of R^{max}_{TX}. This is because, the transmission power may have an unusual increase due to a (unusual) movement of the users at some time step t_p and, hence, such an unusual increase in the transmission power should not affect the evaluation of R^{max}_{TX} at every time step t_k with $p < k$. Next, we use the calculated T^{max}_{TX} at t_k to determine $P_{pr,th}$ at t_k. Since the transmission power is estimated to reach the maximum limit of P^{max}_{TX} in the time T^{max}_{TX}, the time when the battery depletes completely should not occur within the next T^{max}_{TX} seconds. Thus, we choose to fulfill the following condition:

$$\frac{E_b(t_0) - E_b(t_k)}{P_{pr,th}(t_k) + P_{TX}(t_k)} \ge T^{max}_{TX}, \quad (24)$$

or equivalently, $P_{pr,th}(t_k) \leq \frac{E_b(t_0)-E_b(t_k)}{T_{TX}^{max}} - P_{TX}(t_k)$. Hence, we set the value of $P_{pr,th}(t_k)$ to $\frac{E_b(t_0)-E_b(t_k)}{T_{TX}^{max}} - P_{TX}(t_k)$ to tackle the constraint on the FlyBS's battery (i.e., constraint (c) in (8)).

D. Clustering of users for NOMA

In the previous subsection, $X_{cto}^G(t_k)$ and $Y_{cto}^G(t_k)$ are derived as functions of the selected clustering G. Hence, evaluating the transmission power $P_{TX}^{min}(G, t_k)$ at the optimal position is enough to find the optimum clustering G_{opt} to solve the optimization problem in (10).

The naive approach to find the optimum clustering is to evaluate $P_{TX}(X_{cto}^G, Y_{cto}^G, t_k)$ for every possible clustering (i.e., to perform an exhaustive search) and, then, to select the clustering with the smallest corresponding $P_{TX}(X_{cto}^G, Y_{cto}^G, t_k)$. However, the number of all possible clustering options can be very large (there are $\prod_{i=1}^{N_{cl}} \binom{N_u - \sum_{j=0}^{i-1} N_{cu,j}}{N_{cu,i}}$ different clustering options for every set of the cluster sizes $\{N_{cu,1}, ..., N_{cu,cl}\}$). Hence, the exhaustive search is not a practical solution for real word applications. In order to address this issue, we reduce the search space size of the problem by characterizing the optimal clustering function. To this end, we first derive the optimal clustering function G_{opt} via Theorem 1 that provides a necessary condition for G_{opt}.

Theorem 1. *Suppose that before clustering of the users, the x-coordinates of the users are sorted as $X_{sorted} = \{x_{l_1}, \ldots, x_{l_{N_u}}\}$, such that $x_{l_1} < ... < x_{l_{N_u}}$. Also, let N_{cu}^{max} and N_k denote the size of the largest cluster and the number of clusters with a size of k, respectively. Then, for the clustering function that minimizes $P_{TX}(X_{cto}^G, Y_{cto}^G, t_k)$ for a given N_{cu}^{max}, the first users in each cluster with a size of N_{cu}^{max} should be $N_{N_{cu}^{max}}$ consecutive users in the sorted sequence X_{sorted}. Similarly, the set including the $(N_{cu,j}-i+1)$-th user of the j-th cluster ($1 \leq i \leq N_{cu}^{max}$, $j \in \langle 1, N_{cl} \rangle$) should be $\sum_{s=1}^{N_{cu}^{max}-i+1} N_{i+s-1}$ consecutive users in the sorted sequence X_{sorted} after eliminating the selected $(N_{cu,j}-r+1)$-th users of the j-th cluster ($1 \leq r \leq N_{cu}^{max} - i$).*

Proof. See Appendix A.

In addition to Theorem 1, we also define the following proposition that helps us to further reduce the complexity of the user clustering.

Proposition 1. *All permutations of the users $u_{i,j}^G$ with the same value for $(N_{cu,j}-i)$ along all clusters result in different groupings with the same corresponding $P_{TX}(X, Y, H, t_k, G)$.*

Proof. Suppose that for the grouping function G_1, the users $u_{i,j}^{G_1}$ and $u_{i',j'}^{G_1}$ satisfy $N_{cu,j}-i = N_{cu,j'}-i'$. Also, suppose that the grouping function G_2 is derived by exchanging $u_{i,j}^{G_1}$ and $u_{i',j'}^{G_1}$ between the clusters j and j' (i.e., $u_{i',j'}^{G_2} = u_{i,j}^{G_1}$). Since the FlyBS's distance to the users does not change by modifying the grouping (i.e., $d_{i',j'}^{G_2} = d_{i,j}^{G_1}$), from (15), it is concluded that $P_{TX}(X, Y, H, t_k, G_1) = P_{TX}(X, Y, H, t_k, G_2)$. □

Theorem 1 and Proposition 1 together allow to choose the optimal clustering function. In particular, we collect all different clustering options that meet the necessary conditions in Theorem 1, while Proposition 1 enables to avoid collecting the clustering options that lead to the same transmission power. We first find all possible solutions to $\sum_{r=1}^{N_{cl}} N_{cu,r} = N_u$, where $1 \leq N_{cu,r} \leq N_{cu}^{max}$ as follows. We start with checking the necessary conditions for the equation $\sum_{r=1}^{N_{cl}} N_{cu,r} = N_u$ to obtain the solutions satisfying $1 \leq N_{cu,r} \leq N_{cu}^{max}$. By evaluating $\sum_{r=1}^{N_{cl}} N_{cu,r}$ at the upper and lower bounds in $1 \leq N_{cu,r} \leq N_{cu}^{max}$, we get the necessary conditions $N_{cl} \times N_{cu}^{max} \geq N_u$ and $N_{cl} \leq N_u$, respectively. Next, we consider all possible values 1, …, N_{cu}^{max} for $N_{cu,1}$ and, for each of those values, we rewrite our main equation as $\sum_{r=2}^{N_{cl}} N_{cu,r} = N_u - N_{cu,1}$. For the updated equation (with $N_{cl}-1$ variables) we check again the necessary conditions for an existence of solution and eliminate those equations that do not fulfill the conditions. Then we consider all N_{cu}^{max} possible values 1, …, N_{cu}^{max} for $N_{cu,2}$ and update the equation similarly as in the previous step. We repeat the same process and collect all solutions for $\{N_{cu,1}, \ldots, N_{cu,cl}\}$ until the necessary conditions are not held anymore. Then, for every set of the solutions (i.e., sizes of the clusters), we find and collect all clustering candidate options derived from Theorem 1. More specifically, we sort the x-coordinates of the users as $x_{l_1} < ... < x_{l_{N_u}}$, and choose $N_{N_{cu}^{max}}$ consecutive elements from the sorted sequence. Therefore, instead of considering all $\binom{N_u}{N_{N_{cu}^{max}}}$ possible subsets, we only have $(N_u - N_{N_{cu}^{max}} + 1)$ options. According to Proposition 1, for each selected sequence, all permutations result in the same corresponding transmission power. Thus, we only keep one of many permutations for each sequence. According to Theorem 1 a similar process to the previous step is considered, i.e., the i-th users of all clusters with a size of N_{cu}^{max} are chosen together with the $(i-1)$-th users of the clusters with a size of $N_{cu}^{max}-1$ together with the $(i-2)$-th users of the clusters with a size of $N_{cu}^{max}-2$ and so on. This procedure is continued until all users are assigned to clusters. We repeat the same process for all different sizes of clusters, and we collect all the clustering candidates. Then, the transmission power corresponding to every clustering is derived via Algorithm 1. Then, the clustering that yields the minimum transmission power is chosen and applied for NOMA. For every set of the clusters size $\{N_{cu,1}, ..., N_{cu,cl}\}$, the search space size in the proposed clustering is $\prod_{i=1}^{N_{cu}^{max}} (N_u - \sum_{j=0}^{i-1} N_{N_{cu}^{max}-j} + 1)$. The total complexity of the proposed solution is then calculated by summing the complexity over all derived sets of the clusters size $\{N_{cu,1}, ..., N_{cu,cl}\}$. For the exhaustive search, there are $\prod_{i=1}^{N_{cl}} \binom{N_u - \sum_{j=1}^{i-1} N_{cu,j}}{N_{cu,i}}$ different clustering options for every set of the cluster size $\{N_{cu,1}, ..., N_{cu,cl}\}$. Thus, the number of options for the exhaustive search becomes extremely large for realistic values of N_u. For example, for $N_{cu}^{max} = 2$ and $N_{cl} = 7$, the search space for the exhaustive search is about

17.2 million options, whereas the proposed solution leads to only 8 options to be checked. This illustrates significant lowering of the complexity by the proposed solution compared to the exhaustive search.

E. Discussion of optimality of the proposed solution

There is no general way to find the optimal solution to the non-convex problem in (10). Hence, we choose the exhaustive search to show the optimality of the proposed solution. Note that, since there are continuous-valued variables in (10), even performing the exhaustive search cannot achieve the exact optimum. Nevertheless, using the exhaustive search allows us to evaluate the maximum possible gap between the derived transmission power from the proposed solution and the optimal transmission power. We do this evaluation via a combination of a discretized exhaustive search and an analysis of the error caused by the discretization. For the discretized exhaustive search, at every time step, we check all possible user clustering options of the users for NOMA, and we find the minimum corresponding transmission power for each clustering option by finding the optimal values of the acceleration and the velocity of the FlyBS. In particular, at every time step t_k, we consider all possible vectors of the FlyBS's acceleration $\boldsymbol{a}_{FlyBS}(t_k) = (a^x_{FlyBS}(t_k), a^y_{FlyBS}(t_k))$ that fulfill the constraint (e) in (10). For the discretized interval of $[-a^{max}_{FlyBS}, a^{max}_{FlyBS}]$ we consider the values starting with $-a^{max}_{FlyBS}$ and increasing with a step size of ξ. Then, for each selected value of, e.g., φ for $a^x_{FlyBS}(t_k)$ from the discretized interval, the value of $a^y_{FlyBS}(t_k)$ should be within the range of $[-\sqrt{{a^{max}_{FlyBS}}^2 - \varphi^2}, \sqrt{{a^{max}_{FlyBS}}^2 - \varphi^2}]$ to meet the constraint (e) in (10). A similar discretization for the interval $[-\sqrt{{a^{max}_{FlyBS}}^2 - \varphi^2}, \sqrt{{a^{max}_{FlyBS}}^2 - \varphi^2}]$ with a step size of ξ is done to find all possible numerical combinations for the acceleration vector. Then, for each possible acceleration vector, we calculate the vector of velocity from (9). For those velocity vectors fulfilling the constraints (c) and (d) in (10), we calculate the FlyBS's position from (19). Next, at the calculated position of the FlyBS, the corresponding transmission power is derived. We repeat this procedure for values of the acceleration vector and for every clustering option. In the following Lemma 2, we define the upper bound for the discretization error for every tested pair $(a^x_{FlyBS}(t_k), a^y_{FlyBS}(t_k)) = (\varphi, \tau)$ over the discretized sets.

Lemma 2. *The maximum error due to discretization of the interval for the exhaustive search for the acceleration values for $a^x_{FlyBS} \in (\varphi, \varphi + \xi)$ and $a^y_{FlyBS} \in (\tau, \tau + \xi)$ is:*

$$|\zeta| \leq \xi^2|M_{xx}| + 2\xi^2|M_{xy}| + \xi^2|M_{yy}| = \xi^2(|M_{xx}| + 2|M_{xy}| + |M_{yy}|), \tag{25}$$

where M_{xx}, M_{xy}, and M_{yy} are the supremum of $\frac{\partial^2 P_{TX}}{\partial {a^x_{FlyBS}}^2}$, $\frac{\partial^2 P_{TX}}{\partial a^x_{FlyBS} \partial a^y_{FlyBS}}$, and $\frac{\partial^2 P_{TX}}{\partial {a^y_{FlyBS}}^2}$, respectively, over the interval of $a^x_{FlyBS} \in [\varphi, \varphi + \xi]$ and $a^y_{FlyBS} \in [\tau, \tau + \xi]$.

Proof. See appendix B.

Using the error's upper bound in (25), we evaluate the smallest potential value for the transmission power that can occur for $a^x_{FlyBS} \in (\varphi, \varphi + \xi)$ and $a^y_{FlyBS} \in (\tau, \tau + \xi)$. By collecting the calculated lower bound for the transmission power for every candidate clustering option, we find the lowest bound for the transmission power among all clustering options. The lower bound is evaluated for the transmission power in the our scenario in Section IV to confirm that the proposed solution is very close to the optimum.

F. Feasibility of FlyBS positioning and user NOMA clustering and extension to multiple FlyBSs

No solution to the problem defined in (8) exists if the required transmission power to guarantee C_{min} to all users exceeds the maximum transmission power limit of P^{max}_{TX}. Thus, a necessary and sufficient condition for an existence of a solution to (8) is derived using (15) as:

$$Q\sigma^2(2^{\frac{C_{min}}{B}} - 1)\sum_{j=1}^{N_{cl}}\sum_{i=1}^{N_{cu,j}}\left(2^{\frac{C_{min}}{B}\times(N_{cu,j}-i)}\right)d^{G\ \alpha}_{i,j}(t_k) \leq P^{max}_{TX} \tag{26}$$

Once the condition in (26) is fulfilled there definitely exists a solution to (8). If the condition (26) (and hence the constraints (a) and (b) in (8)) are not fulfilled for a given setting of the communication-related parameters, the only approach to make the problem in (8) feasible is to increase the number of FlyBSs. The multiple FlyBSs allow to split the load degenerated by the users to avoid a violation of the constraint (a) on C_{min}.

With respect to the single-FlyBS scenario, an association of the users to the FlyBSs and management of interference among the FlyBSs should be handled. For the user association, a straightforward way is to associate the users based on the commonly used approaches, e.g., the received signal strength [50] or K-means [49]. Of course, the proposed positioning of the FlyBSs and NOMA user clustering is optimal only for the given association. Furthermore, in the multi-FlyBS scenario, other FlyBSs cause interference to NOMA clusters within other FlyBSs. The interference level depends on the users' location with respect to other FlyBSs. Hence, the FlyBS's positioning and the user clustering should be extended by taking the impact of interference from other FlyBSs into account. The user association makes the problem of the FlyBS's positioning and user's clustering NP-hard in general. Solving such problem optimally is itself a challenging and complex task, thus, we leave it for future research.

IV. Simulations and results

In this section, we provide details of models and simulation settings adopted for evaluation of the proposed solution for NOMA user clustering, power allocation, and FlyBS's positioning. Then, we introduce competitive state-of-the-art algorithms, and we thoroughly analyze the performance of the proposal and demonstrate the advantages of the proposal over the existing solutions.

A. Simulation scenario and models

We consider a scenario where the FlyBS serves users represented by vehicles and/or users in vehicles during a busy traffic or a traffic jam on a road or a highway. In such situation, the FlyBS is a suitable solution to improve the performance of an overloaded network (see, e.g., [39], [40]). The FlyBS is represented by a common rotary-wing UAV. Such UAV can fly typically with a maximum speed of about 25–30 m/s [44]. Thus, the rotary-wing UAV is suitable for our scenario, as the vehicles in the busy traffic or in the traffic jam usually move with speeds within the limits of the common UAV. Following [43], the FlyBS's altitude is fixed at $H = 100$ m.

The users move on a 3-lane highway in the positive direction of the x-axis. The users are distributed uniformly among all three lanes. Within one lane, we set a two-second rule, that is, the minimum safe distance between two vehicles is equal to the distance moved by the vehicles within two seconds. This rule is adopted and suggested for a driving in the real world to roughly maintain a safe distance between the vehicles, while also taking the speed of vehicles into account to specify the minimum distance between the vehicles over time. Furthermore, the speeds are selected uniformly over the intervals {14-16} m/s, {14-17} m/s, and {15-19} m/s for the first, second, and third lanes, respectively. The range of vehicles' speeds is selected considering the maximum flying speed of the FlyBS, as the FlyBS should be able to fly with the served vehicles with a certain speed margin to adjust a relative position with respect to the vehicles. Note that the FlyBS knows the location of users only with a measurement error $e^x_{i,j}$ and $e^x_{i,j}$ uniformly distributed over $[-10, 10]$ m at every time step.

To validate the assumption on the LoS communication, we evaluate the probability of LoS in our scenario as follows. We first solve the problem of the FlyBS's positioning with the assumption of LoS transmission to all the users. Then, we calculate the LoS occurrence (defined by 60% of the first Fresnel zone to be clear of obstacles) in the modeled suburban environment. In line with [47], we assume that the average height, width, and length of the buildings are set to 15 m and the density of the buildings is 13% of the total area. The height of the users' receiving antenna is set to 1.5 m. According to our simulations, the average probability of LoS is 99.6%, 99.1%, and 98.4% in the scenarios with 30, 60, and 90 users, respectively.

The simulations are commonly performed for $C_{min} = 15$ Mbps by each user, however, we also analyze the impact of C_{min} on the performance. Each simulation is of 1200 seconds duration with the user clustering and the transmission power calculated every 0.1 seconds. The results are averaged out over 100 simulation drops. The system parameters are summarized in Table I.

Our proposed solution is investigated for two cases: i) *Communication coverage-maximizing clustering and FlyBS's positioning* (CMCP) for NOMA, as elaborated in Section III and with setting of $V_{th,1} = 12$ m/s, $V_{th,2} = 33$ m/s (see (10)), and ii) *Propulsion power minimization (PPM)*, which is a specific case of the proposed solution with the setting minimizing the propulsion power consumption, i.e., with $V_{th,1} = V_{th,2} = 22.7$ m/s and $P_{pr,th} = 461.6$ W. Both options are compared with the following related state-of-the-art schemes:

i) *Sum rate maximization (SRM)* algorithm, introduced in [18], that provides a joint NOMA pairing and FlyBS's positioning for sum rate maximization. Note that the SRM algorithm does not include the constraints on the speed and acceleration in (10). Thus, for a fair comparison, we adjust the FlyBS's speed and acceleration to the closest value within the allowed range in case that the required speed or acceleration exceed their limits.

ii) *enhanced SRM (ESRM)* algorithm that adopts the pairing scheme proposed in [18], but the positioning of FlyBS is enhanced by our proposed optimal positioning in order to reduce the transmission power, as the solution proposed in [18] targets to maximize the sum rate,

iii) *NOMA for static base station (SBS)*, developed in [46], that maximizes the sum capacity for static base station and, hence, does not provide any solution to the FlyBS's positioning,

iv) *enhanced SBS (ESBS)*, that exploits the clustering scheme adopted in [46], and is enhanced with our proposed optimal positioning of the FlyBS to avoid limitations implied by the static base station assumed in [30].

TABLE I: Parameter Configurations

System Parameter	Numerical value
Number of users, N_u	{30,60,90}
FlyBS's antenna gain, $D^{j,TX}_{i,G}$	7 dBi [45]
User's antenna gain, $D^{j,R}_{i,G}$	0 dBi [45]
Noise power spectral density, N_i	–174 dBm/Hz
RF frequency, f	2.6 GHz
System bandwidth	100 MHz
Altitude of FlyBS, H	100 meters
User's required capacity, C_{min}	{10,12,15,18,20} Mbps

B. Simulation results

In this subsection, we present and discuss simulation results. First, we focus on an evolution of the FlyBS's transmission power consumption over time to demonstrate the advantage of our proposal over the existing solutions in terms of efficiency in transmission power management and consequent enhancement of the NOMA communication coverage. We also compare the performance of the proposed scheme with existing solutions in terms of complexity, average transmission power, maximum potential common capacity, and average propulsion power for various numbers of users (N_u), and minimum required capacities by each user (C_{min}). Furthermore, we evaluate the performance of the proposed solution for different maximum cluster sizes N^{max}_{cu}.

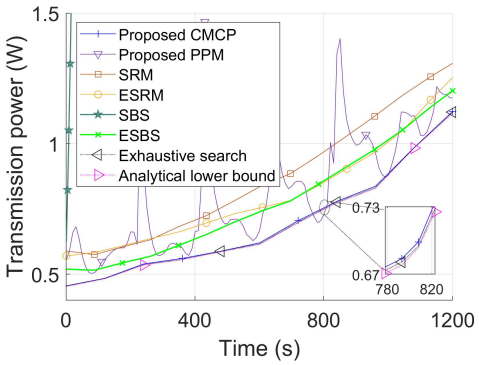

Fig. 4: Transmission power vs. operation time for $N_u = 90$ and $C_{min} = 15$ Mbps. Only part of the values for SBS are shown, as the transmission power is in the order of hundreds of watts.

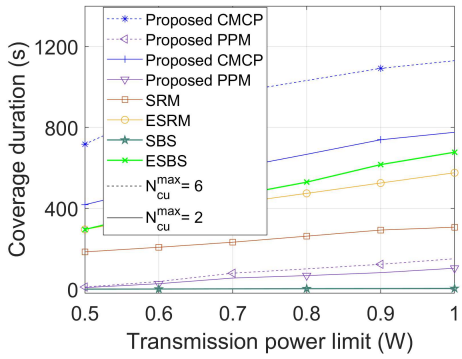

Fig. 5: Duration of communication coverage vs. transmission power limit for different methods and $N_u = 90$ and $C_{min} = 15$ Mbps.

Fig. 4 illustrates an evolution of the transmission power of the FlyBS over time for $C_{min} = 15$ Mbps and for $N_u = 90$. In this figure, we assume NOMA user pairing ($N_{cu}^{max} = 2$, $N_{cl} = 45$) for all existing solutions as these do not allow $N_{cu}^{max} > 2$. In general, the transmission power consumption is increasing over time for all solutions. This is due to a general increase in the relative distance between the first and the last vehicles in the scenario over time, caused by diverse velocities of the vehicles on different lanes, leading to a gradual expansion of the area demarcated by the users. Fig. 4 further shows that the transmission powers corresponding to SRM, ESRM, SBS, and ESBS grow notably faster than for our proposed solution. This faster growth of the transmission power in the existing solutions is due to the sub-optimality of the user clustering in SRM, ESRM, SBS, and ESBS. Furthermore, it is observed that PPM leads to frequent peaks in the transmission power. These peaks are due to the fact that the FlyBS's speed is set to minimize the propulsion power and consequent limitation of the FlyBS's ability in reaching a suitable position at desired time step.

According to Fig. 4, after 1200 s the proposed positioning of the FlyBS applied to SRM (towards ESRM) reduces the transmission power by 6% comparing to the original positioning proposed for the existing SRM. Another notable reduction of up to 5% and 10% compared with the transmission power in ESRM and ESBS, respectively, is achieved by our proposed solution considering a joint positioning of the FlyBS, optimal allocation of transmission power, and optimal user pairing. In total, the proposed solution reduces the transmission power with respect to the original state-of-the-art solutions SRM and SBS by 15% and 99.95%, respectively. In addition, Fig. 4 shows the transmission power over time for the exhaustive search over the discretized intervals and also the lower bound calculated analytically according to (25). The gap between the transmission power achieved by the proposed CMCP and the exhaustive search is typically lower than 0.15%, and always below 1%. Furthermore, the gap between the results from CMCP and the analytical lower bound is typically lower than 0.2% and always below 1.5%. This small difference demonstrates that the performance of the (suboptimal) proposed solution is very close to the optimal solution.

Next, the coverage duration ($T_{coverage}$ as defined in subsection II.B) achieved by the proposed and competitive schemes is depicted in Fig. 5. The figure shows that the proposed scheme significantly enhances the duration of communication coverage with C_{min} guaranteed to all users. If the transmission power of the FlyBS is limited to 1 Watt (i.e., $P_{TX}^{max} = 1$ W), the FlyBS guarantees C_{min} to all users only for 104 s, 5 s, 677 s, 306 s, and 575 s, for PPM, SBS, ESBS, SRM, and ESRM, respectively. As an impact of the proposed FlyBS's positioning, the duration of NOMA communication coverage in ESRM and ESBS is 42% and 7620% higher than in SRM and SBS, respectively. For pairing ($N_{cu}^{max} = 2$), the proposed combined optimal clustering and optimal FlyBS's positioning further enhances the coverage duration by 35% and 14% comparing to ESRM and ESBS, respectively. Moreover, Fig. 5 also shows an impact of the cluster size, as proposed for CMCP and PPM. The proposed extension of the cluster size to $N_{cu}^{max} = 6$ further prolongs the communication coverage duration of the proposed CMCP by 648%, 96% and 67% with respect to PPM, ESRM and ESBS, respectively. This superior performance is a result of the joint optimization of clustering, power allocation, and positioning of the FlyBS. Note that the coverage duration for PPM is significantly lower than for CMCP, ESRM, and ESBS due to the peaks in the transmission power during the operation (as observed in Fig. 4). Also, the transmission power reached by SBS rises very quickly and it becomes in the order of hundreds of watts after few tens of seconds, since the relative distance between the base station and the users increases notably due to immobility of the static base station. Hence, the results for the SBS are not included in further plots and we illustrate only the results for ESBS which enhances the SBS with our proposed FlyBS's positioning.

We also discuss the impact of the cluster size on the transmission power for the proposed CMCP and PPM in Fig. 6. According to Fig. 6, the average transmission power decreases by increasing the maximum number of users grouped in the cluster (i.e., N_{cu}^{max}). The decrease is getting

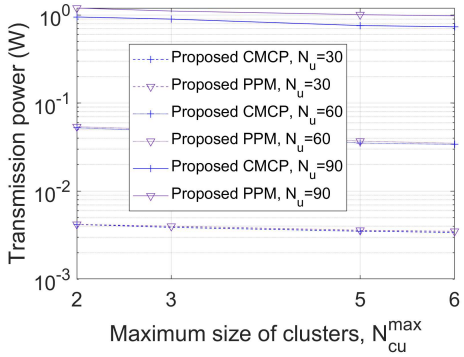

Fig. 6: Average transmission power vs. N_{cu}^{max} for $N_u = 30, 60, 90$, and $C_{min} = 15$ Mbps, for CMCP and PPM.

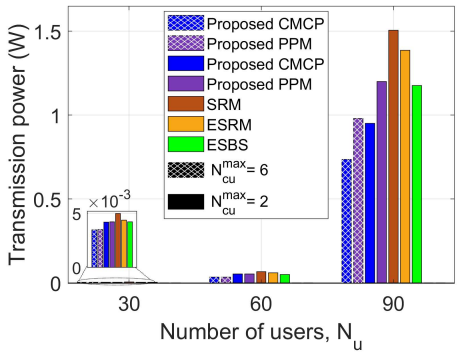

Fig. 7: Average transmission power vs. number of users for different schemes and $C_{min} = 15$ Mbps.

less significant, and the average transmission power saturates with larger N_{cu}^{max} so that the difference between $N_{cu}^{max} = 5$ and $N_{cu}^{max} = 6$ becomes marginal. This saturation is caused by a stronger interference among users in the same cluster if the cluster is of a larger size. Furthermore, the proposed CMCP reduces the transmission power with respect to the PPM by 3%, 6%, and 34% for $N_u = 30$, $N_u = 60$, and $N_u = 90$, respectively.

Next, we investigate the impact of the number of users on the FlyBS's transmission power in Fig. 7. The average transmission power increases with the number of users N_u, as a larger N_u results in a less bandwidth available for each cluster of users. Consequently, a higher transmission power is required to satisfy the required C_{min} for every user. Our proposed solution reaches the lowest transmission power disregarding the number of served users. The highest transmission power is required by the state-of-the-art schemes SRM and SBS. The transmission power is notably reduced by 8% and 99.9% (for $N_u = 90$) by applying our proposed positioning of the FlyBS on the top of the original SRM and SBS towards ESRM and ESBS, respectively. Further significant improvement of 31% and 19% with respect to ESRM and ESBS, respectively, is achieved by our proposal considering joint positioning of the FlyBS, optimal allocation of transmission power, and optimal user clustering (with $N_{cu}^{max} = 2$). Thus, the proposed solution reduces the transmission power with respect to the original state-of-the-art solutions SRM and SBS by 37% and 99.96%, respectively. In addition, by an extension of the cluster size to $N_{cu}^{max} = 6$, the proposed CMCP reduces the transmission power with respect to CMCP with $N_{cu}^{max} = 2$ by 23%. Thus, in total, the proposed CMCP with $N_{cu}^{max} = 6$ reduces the transmission power with respect to SRM and SBS by 47% and 99.97%, respectively.

We show also the FlyBS's propulsion power consumption in Fig. 8. The propulsion power for PPM is lower than all other schemes due to the setting of the propulsion power threshold ($P_{pr,th}$) to the minimum propulsion power. The figure shows that, for $N_u = 30$ and $N_u = 60$, the propulsion power required by the schemes where the proposed positioning is applied (i.e., CMCP, PPM, ESRM, and ESBS) is close to each other (the

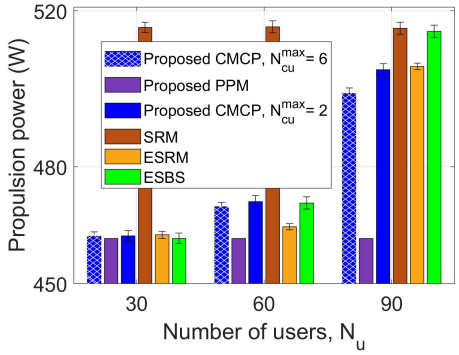

Fig. 8: Average propulsion power consumed by FlyBS vs. number of users for different schemes and $C_{min} = 15$ Mbps.

difference among those schemes is less than 2.5% with the confidence interval of 95%). This is due to the fact that the transmission power is so low for $N_u = 30$ and $N_u = 60$ that the proposed positioning of the FlyBS enhances the coverage duration via the propulsion power reduction (by reducing $P_{pr,th}$) rather than via the transmission power reduction. As a result of such strategy, the propulsion power consumption for CMCP, ESRM, and ESBS becomes similar to PPM.

Next, we investigate the impact of the minimum required capacity C_{min} on the transmission power in Fig. 9. The transmission power for all approaches increases with C_{min} as expected according to (15). Nevertheless, the sub-optimality of the user clustering in the existing state-of-the-art solutions results in a significantly higher rise in the transmission power comparing to our proposed scheme. According to Fig. 9, the proposed CMCP (with $N_{cu}^{max} = 2$) brings up to 47%, 50%, 45%, 100%, and 31% reduction in the transmission power consumption comparing to PPM, SRM, ESRM, SBS, and ESBS, respectively. Furthermore, by the extension of CMCP to the cluster size of $N_{cu}^{max} = 6$, the transmission power is reduced by another 41% with respect to CMCP with $N_{cu}^{max} = 2$. Moreover, the transmission power for PPM is also enhanced by 37% via the extension of $N_{cu}^{max} = 2$ to $N_{cu}^{max} = 6$. Overall, the proposed CMCP (with $N_{cu}^{max} = 6$) brings up to 38%, 70%, 67%, 100%, and 59% reduction in the

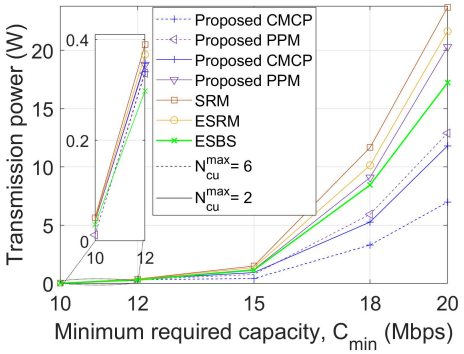

Fig. 9: Average transmission power vs. C_{min} for different algorithms and $N_u = 90$.

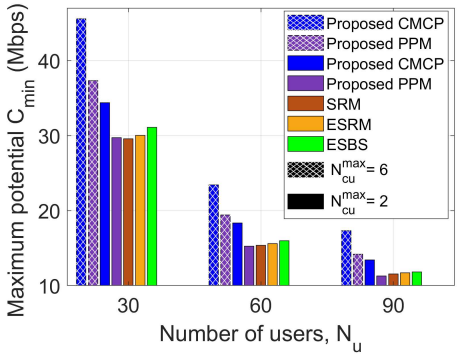

Fig. 10: Maximum potential C_{min} with a fixed transmission power consumption of $P_{fixed}^{G,TX} = 1$ W.

TABLE II: Complexity of the transmission power optimization represented as the number of math operations required to obtain results for user pairing ($N_{cu}^{max} = 2$).

Approach	$N_u = 30$	$N_u = 60$	$N_u = 90$
Proposed CMCP	16	31	46
ESRM	30	60	90
Exhaustive search	2×10^{20}	3.1×10^{49}	1.2×10^{82}

transmission power consumption comparing to PPM, SRM, ESRM, SBS, and ESBS, respectively. It is also noted that, the proposed solution presents realistic values for the transmission power in Fig. 9 ([44], [48]).

We also determine the maximum potential C_{min} for the given transmission power $P_{fixed}^{G,TX} = 1$ W in Fig. 10. For $N_{cu}^{max} = 2$, the proposed CMCP increases the maximum potential C_{min} by up to 19%, 13%, 14%, and 16% compared to PPM (with $N_{cu}^{max} = 2$), ESBS, ESRM, and SRM, respectively. Considering also the proposed extension of the NOMA cluster size to $N_{cu}^{max} = 6$, the proposed CMCP improves the maximum potential C_{min} by 53%, 46%, 48%, and 50% compared with PPM (with $N_{cu}^{max} = 6$), ESBS, ESRM, and SRM, respectively.

We further show the maximum potential C_{min} of the proposed CMCP for the scenario with multiple FlyBSs in Fig. 11. We consider the users association based on K-means [49] and orthogonal resources allocated to the FlyBSs. The available bandwidth $N_u \times B$ is split between the FlyBSs proportionally to the number of associated users to each FlyBS. We observe that the maximum potential C_{min} increases with the number of FlyBSs, since the number of associated users to each FlyBS decreases and, at the same time, also the average distance between the FlyBSs and the users decreases. The maximum potential C_{min} reached by single FlyBS is enhanced by 7% and 16% for 2 and 3 FlyBSs, respectively, for both for $N_{cu}^{max} = 2$ as well as $N_{cu}^{max} = 6$. Such an increase in the maximum potential C_{min} confirms that an infeasible guarantee of C_{min} for single FlyBS in (8) can become feasible for a higher number of adopted FlyBSs.

Last, we also compare the complexity of the proposed and state-of-the-art solutions for user pairing in Table II. For each

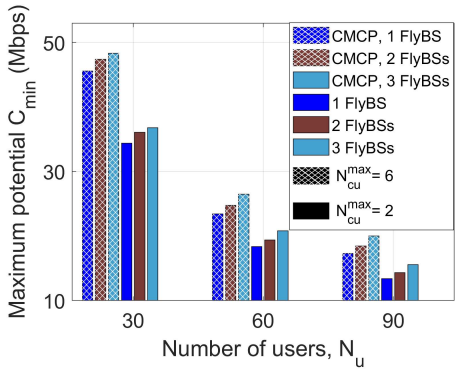

Fig. 11: Maximum potential C_{min} for the proposed CMCP for N_u =30, 60, 90 for 1, 2, and 3 FlyBSs.

value of N_u the comparison between different algorithms is done under the same number of clusters. The complexity is defined as the number of calculations (math operations) performed by each solution. The complexity of the proposed CMCP can be calculated as explained in Subsection III.D, and the computational complexity of ESRM is linear with respect to N_u. The results are shown for $N_{cu}^{max} = 2$, since ESRM is designed for $N_{cu}^{max} = 2$, and its extension to $N_{cu}^{max} > 2$ is not straightforward. Note that we do not include the complexity of SRM, SBS, or ESBS, as the complexity of these are not easy to calculate. The reason is that the SRM solution is based on bisection search [18], and its complexity is even higher than for ESRM. In SBS and ESBS, the power allocation and clustering are derived using convex optimization [30] for which the complexity cannot be easily determined. Table II confirms that the proposed scheme reduces the complexity significantly with respect to the exhaustive search (1.26×10^{19} times, 10^{48} times, and 2.7×10^{80} times for $N_u = 30$, $N_u = 60$, and $N_u = 90$, respectively), and it is even lower than the complexity of ESRM.

V. Conclusions

In this paper, we have studied the problem of joint optimization of user clustering, transmission power allocation, and FlyBS's positioning in future mobile networks based on

NOMA. We formulate the transmission power optimization problem in terms of the clustering of users for NOMA purposes, and the positioning of the FlyBS over time as the users move. Then, we provide a solution to find the optimum clustering of users, and the FlyBS's positions that yield the minimum transmission power while guaranteeing a minimum required capacity for all users. This allows a significant increase in the NOMA communication coverage duration for the FlyBS. We show that the proposed solution extends the FlyBS's coverage duration by tens of percent.

In the future work, the scenario with multiple FlyBS should be studied. This scenario implies another dimension of the problem related to the user association to individual FlyBSs as well as a management of interference from the FlyBSs [49], [50]. Furthermore, the problem of optimal bandwidth allocation should be considered.

APPENDIX A
PROOF TO THEOREM 1

Proof. We prove Theorem 1 using mathematical contradiction as follow: Let $N_{cl,i}$ denote the number of clusters of a size i. Also, let $cl_{j_1}, ..., cl_{j_{N_{cl,N_{cu}^{max}}}}$ be the clusters of a size N_{cu}^{max}. Suppose that $\{x_{1,cl_{j_1}}^{G_{opt}}, x_{1,cl_{j_2}}^{G_{opt}}, \ldots, x_{1,cl_{j_{N_{cl,N_{cu}^{max}}}}}^{G_{opt}}\} = \{x_{i_1}, ..., x_{i_{N_{cl,N_{cu}^{max}}}}\}$ with $x_{i_1} < ... < x_{i_{N_{cl,N_{cu}^{max}}}}$. Then, by contradiction, we assume that the users in $\{x_{i_1}, ..., x_{i_{N_{cl,N_{cu}^{max}}}}\}$ are not consecutive in X_{sorted}, and there exists x_j such that $x_{i_1} < x_j < x_{i_{N_{cl,N_{cu}^{max}}}}$ and $x_j \notin \{x_{i_1}, ..., x_{i_{N_{cl,N_{cu}^{max}}}}\}$. Also, we assume that, for G_{opt}, x_j is the s-th user in some cluster ($s > 1$). Let G_1 denote the clustering function that is obtained by swapping x_{i_1} and x_j in G_{opt}. Similarly, G_2 denotes the clustering obtained by swapping $x_{i_{N_{cl,N_{cu}^{max}}}}$ and x_j in G_{opt}. From the optimality of G_{opt} it is inferred that:

$$\begin{aligned} &P_{TX}(X,Y,H,t_k,G_{opt})|_{(X_{cto}^{G_{opt}},Y_{cto}^{G_{opt}})} - \\ &P_{TX}(X,Y,H,t_k,G_1)|_{(X_{cto}^{G_{opt}},Y_{cto}^{G_{opt}})} < 0, \\ &P_{TX}(X,Y,H,t_k,G_{opt})|_{(X_{cto}^{G_{opt}},Y_{cto}^{G_{opt}})} - \\ &P_{TX}(X,Y,H,t_k,G_2)|_{(X_{cto}^{G_{opt}},Y_{cto}^{G_{opt}})} < 0. \end{aligned} \tag{27}$$

Now, we rewrite the left-hand side terms in (27) by means of the system parameters as follow:

$$\begin{aligned} &P_{TX}(X,Y,H,t_k,G_{opt})|_{(X_{cto}^{G_{opt}},Y_{cto}^{G_{opt}})} - \\ &P_{TX}(X,Y,H,t_k,G_1)|_{(X_{cto}^{G_{opt}},Y_{cto}^{G_{opt}})} = \\ &\gamma_{min} Q \sigma^2 \big((1+\gamma_{min})^{N_{cu}^{max}-1} - (1+\gamma_{min})^{N_{cu}^{max}-s}\big)({d_{i_1}}^{\alpha} - {d_j}^{\alpha}), \\ &P_{TX}(X,Y,H,t_k,G_{opt})|_{(X_{cto}^{G_{opt}},Y_{cto}^{G_{opt}})} - \\ &P_{TX}(X,Y,H,t_k,G_2)|_{(X_{cto}^{G_{opt}},Y_{cto}^{G_{opt}})} = \\ &\gamma_{min} Q \sigma^2 \big((1+\gamma_{min})^{N_{cu}^{max}-1} - (1+\gamma_{min})^{N_{cu}^{max}-s}\big)(d_{i_{N_{cl,N_{cu}^{max}}}}^{\alpha} - {d_j}^{\alpha}) \end{aligned} \tag{28}$$

From the first inequality in (27) and the first equality in (28) it is included that $(d_{i_1} - d_j) < 0$. Similarly, from the second inequality in (27) and the second equality in (28) it is concluded that $(d_{i_{N_{cl,N_{cu}^{max}}}} - d_j) < 0$. However, the inequalities $(d_{i_1} - d_j) < 0$ and $(d_{i_{N_{cl,N_{cu}^{max}}}} - d_j) < 0$ cannot hold at the same time given the assumption that $x_{i_1} < x_j < x_{i_{N_{cl,N_{cu}^{max}}}}$ due to following reasons. First, in a movement on a road in the direction of the x-axis, the range of x-coordinates of the users is much larger than the range of y-coordinates. Thus, from $(d_{i_1} - d_j) < 0$ it is concluded that $X_{cto} < \frac{(x_{i_1}+x_j)}{2}$. Similarly, from $(d_{i_{N_{cl}}} - d_j) < 0$ it is concluded that $X_{cto} > \frac{(x_{i_{N_{cl,N_{cu}^{max}}}}+x_j)}{2}$. By incorporating the two derived inequalities $X_{cto} < \frac{(x_{i_1}+x_j)}{2}$ and $X_{cto} > \frac{(x_{i_{N_{cl,N_{cu}^{max}}}}+x_j)}{2}$ we get $x_{i_1} > x_{i_{N_{cl,N_{cu}^{max}}}}$, which contradicts the assumption of $x_{i_1} < x_{i_{N_{cl,N_{cu}^{max}}}}$. Hence, the initial assumption that the users in $\{x_{1,cl_{j_1}}^{G_{opt}}, x_{1,cl_{j_2}}^{G_{opt}}, \ldots, x_{1,cl_{j_{N_{cl,N_{cu}^{max}}}}}^{G_{opt}}\}$ are not consecutive is incorrect. Therefore, $\{x_{i_1}, ..., x_{i_{N_{cl,N_{cu}^{max}}}}\}$ consists of the consecutive users in X_{sorted}. By a similar procedure as above, we verify that the second users of the clusters of a size N_{cu}^{max} and the first users of the clusters of a size $N_{cu}^{max} - 1$ should be consecutive values in X_{sorted} after eliminating $\{x_{1,cl_{j_1}}^{G_{opt}}, x_{1,cl_{j_2}}^{G_{opt}}, \ldots, x_{1,cl_{j_{N_{cl,N_{cu}^{max}}}}}^{G_{opt}}\}$, and so on so forth for the next users of all clusters. This completes the proof to Theorem 1. □

APPENDIX B
PROOF OF LEMMA 2

Proof. To determine the discretization error in the exhaustive search we use the first-derivative Taylor approximation with respect to a_{FlyBS}^x and a_{FlyBS}^y. Then, the approximation error (denoted by ζ) is expressed in terms of the second derivatives, i.e.,

$$\begin{aligned} \zeta = (a_{FlyBS}^x - \varphi)^2 \frac{\partial^2 P_{TX}}{\partial {a_{FlyBS}^x}^2}|_{(X(\varphi^+),Y(\tau^+))} + \\ (a_{FlyBS}^y - \tau)^2 \frac{\partial^2 P_{TX}}{\partial {a_{FlyBS}^y}^2}|_{(X(\varphi^+),Y(\tau^+))} + \\ 2(a_{FlyBS}^x - \varphi)(a_{FlyBS}^y - \tau) \frac{\partial^2 P_{TX}}{\partial a_{FlyBS}^x \partial a_{FlyBS}^y}|_{(X(\varphi^+),Y(\tau^+))} \end{aligned} \tag{29}$$

where φ^+ and τ^+ are (unknown) values satisfying $\varphi^+ \in [\varphi, \varphi+\xi]$ and $\tau^+ \in [\tau, \tau+\xi]$. Using the triangle inequality, and by the fact that $0 \le a_{FlyBS}^x - \varphi \le \xi$ and $0 \le a_{FlyBS}^y - \tau \le \xi$ for $a_{FlyBS}^x \in [\varphi, \varphi+\xi]$ and $a_{FlyBS}^y \in [\tau, \tau+\xi]$, the error is upper bounded by:

$$\begin{aligned} |\zeta| \le \xi^2 |M_{xx}| + 2\xi^2 |M_{xy}| + \xi^2 |M_{yy}| = \\ \xi^2 (|M_{xx}| + 2|M_{xy}| + |M_{yy}|), \end{aligned} \tag{30}$$

□

REFERENCES

[1] B. Li, Z. Fei and Y. Zhang, "UAV Communications for 5G and Beyond: Recent Advances and Future Trends," *IEEE Internet Things J.*, vol. 6, no. 2, 2019.

[2] A. Chriki, H. Touati, H. Snoussi and F. Kamoun, "UAV-GCS Centralized Data-Oriented Communication Architecture for Crowd Surveillance Applications," *IWCMC*, 2019.

[3] A. Puri, "A survey of unmanned aerial vehicles (UAV) for traffic surveillance," January 2005.

[4] J. Lyu, et al., "Placement Optimization of UAV-Mounted Mobile Base Stations," *IEEE Commun. Lett.*, vol. 21, no. 3, 2017.

[5] X. Cheng, et al., "Architecture Design of Communication and Backhaul for UAVs in Power Emergency Communication," *IEEE ICCCBDA* 2019.

[6] X. Li, et al., "A Near-Optimal UAV-Aided Radio Coverage Strategy for Dense Urban Areas," *IEEE Trans. Veh. Technol.*, vol. 68, no. 9, pp. 9098-9109, Sept. 2019.

[7] E. Kalantari, H. Yanikomeroglu, and A. Yongacoglu, "On the number and 3D placement of drone base stations in wireless cellular networks," *IEEE VTC2016-Fall*.

[8] M. Samir, et al., "UAV Trajectory Planning for Data Collection from Time-Constrained IoT Devices," *IEEE Trans. Wireless Commun.*, vol. 19, no. 1, pp. 34-46, Jan. 2020.

[9] L. Wang, "Multiple access mmwave design for UAV-aided 5g communications," *IEEE Wireless Communications*, 2019.

[10] Y. Ji, et al., "Multi-cell Edge Coverage Enhancement Using Mobile UAV-Relay," *IEEE Internet Things Journal*, 2020.

[11] H. Shakhatreh, et al., "Efficient 3D placement of a UAV using particle swarm optimization," *ICICS*, 2017.

[12] X. Liu, J. Miao and P. Wang, "Throughput Optimization of Blocked Data Transmission: A Mobile-Relay-UAV-Assisted Approach," *IEEE ICCC*, 2019.

[13] Z. Wang, L. Duan and R. Zhang, "Adaptive Deployment for UAV-Aided Communication Networks," in *IEEE Trans. Wireless Commun.*, vol. 18, no. 9, Sept. 2019.

[14] M. Nikooroo and Z. Becvar, "Joint Positioning of UAV and Power Control for Flying Base Stations in Mobile Networks," *IEEE WiMOB*, 2019.

[15] M. Nikooroo, Z. Becvar, "Optimizing Transmission and Propulsion Powers for Flying Base Stations," *IEEE WCNC*, 2020.

[16] O. Maraqa, et al., "A survey of rate-optimal power domain noma with enabling technologies of future wireless networks," *IEEE Communications Surveys & Tutorials*, Feb. 2020.

[17] L. Dai, et al., "Non-orthogonal multiple access for 5G: solutions, challenges, opportunities, and future research trends," *IEEE Communications Magazine*, vol. 53, no. 9, pp. 74-81, September 2015.

[18] M. Nguyen and L. Le, "NOMA User Pairing and UAV Placement in UAV-Based Wireless Networks," *IEEE ICC*, 2019.

[19] Z. Ding, et al., "On the Performance of Non-Orthogonal Multiple Access in 5G Systems with Randomly Deployed Users," *IEEE Signal Process. Lett.*, vol. 21, no. 12, Dec. 2014.

[20] K. Chi, Z. Chen, K. Zheng, Y. Zhu and J. Liu, "Energy Provision Minimization in Wireless Powered Communication Networks With Network Throughput Demand: TDMA or NOMA?," *IEEE Trans. Commun.*, vol. 67, no. 9, Sept. 2019.

[21] B. Kim, et al., "Partial Non-Orthogonal Multiple Access (P-NOMA) with Respect to User Fairness," *IEEE VTC2019-Fall*.

[22] S. Timotheou, I. Krikidis, "Fairness for Non-Orthogonal Multiple Access in 5G Systems," *IEEE Signal Process. Lett.*, vol. 22, no. 10, 2015.

[23] M. F. Sohail, C. Y. Leow and S. Won, "Non-Orthogonal Multiple Access for Unmanned Aerial Vehicle Assisted Communication," in *IEEE Access*, vol. 6, pp. 22716-22727, 2018.

[24] J. Kang and I. Kim, "Optimal User grouping for Downlink NOMA," in *IEEE Wireless Commun. Lett.*, vol. 7, no. 5, 2018.

[25] Z. Chen, K. Chi, K. Zheng, Y. Li and X. Liu, "Common Throughput Maximization in Wireless Powered Communication Networks With Non-Orthogonal Multiple Access," *IEEE Trans. Veh. Technol.*, vol. 69, no. 7, July 2020.

[26] Z. Shi, W. Gao, S. Zhang, J. Liu and N. Kato, "Machine Learning-Enabled Cooperative Spectrum Sensing for Non-Orthogonal Multiple Access," *IEEE Trans. Commun.*, vol. 19, no. 9, pp. 5692-5702, Sept. 2020.

[27] W. Peng, W. Gao and J. Liu, "AI-Enabled Massive Devices Multiple Access for Smart City," *IEEE Internet Things Journal*, vol. 6, no. 5, Oct. 2019.

[28] Z. Shi, W. Gao, S. Zhang, J. Liu and N. Kato, "AI-Enhanced Cooperative Spectrum Sensing for Non-Orthogonal Multiple Access," *IEEE Wireless Communications*, vol. 27, no. 2, April 2020.

[29] M. F. Sohail and C. Y. Leow, "Maximized fairness for NOMA based drone communication system," IEEE MICC, 2017.

[30] L. Lei, D. Yuan and P. Värbrand, "On Power Minimization for Non-orthogonal Multiple Access (NOMA)," in *IEEE Commun. Lett.*, vol. 20, no. 12, pp. 2458-2461, Dec. 2016.

[31] A. Nasir, et al., "UAV-Enabled Communication Using NOMA," *IEEE Trans. Commun.*, vol. 67, no. 7, 2019.

[32] P. Sharma, D. Kim, "UAV-Enabled Downlink Wireless System with Non-Orthogonal Multiple Access," *GC Wkshps*, 2017.

[33] J. Baek, S. I. Han and Y. Han, "Optimal Resource Allocation for Non-Orthogonal Transmission in UAV Relay Systems," *IEEE Wireless Commun. Lett.*, vol. 7, no. 3, pp. 356-359, June 2018.

[34] N. Zhao, et al., "Joint Trajectory and Precoding Optimization for UAV-Assisted NOMA Networks," *IEEE Trans. Commun.*, vol. 67, no. 5, pp. 3723-3735, May 2019.

[35] X. Liu, et al., "Placement and Power Allocation for NOMA-UAV Networks," *IEEE Wireless Commun. Lett.*, June 2019.

[36] W. Wang, et al., "Joint Precoding Optimization for Secure SWIPT in UAV-Aided NOMA Networks," *IEEE Trans. Commun.*, vol. 68, no. 8, pp. 5028-5040, Aug. 2020

[37] Xiaowei Pang, et al, "Energy-Efficient Design for mmWave-Enabled NOMA-UAV Networks", *SCI Journal*, 2021.

[38] M. Nikooroo and Z. Becvar, "Optimization of Transmission Power for NOMA in Networks with Flying Base Stations," *IEEE VTC2020-Fall*, 2020.

[39] P. Yang, et al., "Proactive Drone-Cell Deployment: Overload Relief for a Cellular Network Under Flash Crowd Traffic," *IEEE Trans. Intell. Transp. Syst.*, vol. 18, no. 10, pp. 2877-2892, Oct. 2017.

[40] Z. Becvar, et al., "Performance of Mobile Networks with UAVs: Can Flying Base Stations Substitute Ultra-Dense Small Cells?," *European Wireless*, 2017.

[41] K. Senel, H. V. Cheng, E. Björnson and E. G. Larsson, "What Role can NOMA Play in Massive MIMO?," *IEEE J. Sel. Topics Signal Process.*, vol. 13, no. 3, pp. 597-611, 2019.

[42] S. Ahmed, M. Z. Chowdhury and Y. M. Jang, "Energy-Efficient UAV-to-User Scheduling to Maximize Throughput in Wireless Networks," *IEEE Access*, vol. 8, pp. 21215-21225, 2020.

[43] Y. Zeng, J. Xu, and R. Zhang, "Energy Minimization for Wireless Communication With Rotary-Wing UAV," in *IEEE Trans. Wireless Commun.*, Vol. 18, No. 4, April 2019.

[44] A. Fotouhi, et al., "Survey on UAV Cellular Communications: Practical Aspects, Standardization Advancements, Regulation, and Security Challenges," *IEEE Commun. Surveys Tuts.*, vol. 21, no. 4, 2019.

[45] M. Bekhti, et al., "Path planning of unmanned aerial vehicles with terrestrial wireless network tracking," *IEEE WD*, 2016.

[46] L. You and D. Yuan, "A Note on Decoding Order in User Grouping and Power Optimization for Multi-Cell NOMA With Load Coupling," *IEEE Trans. Wireless Commun.*, vol. 20, no. 1, pp. 495-505, Jan. 2021.

[47] J. Turkka and M. Renfors, "Path loss measurements for a non-line-of-sight mobile-to-mobile environment," *International Conference on ITS Telecommunications*, 2008.

[48] "Examples of technical characteristics for unmanned aircraft control and non-payload communications links," *ITU-R,* 2011.

[49] R. Duan, J. Wang, C. Jiang, H. Yao, Y. Ren and Y. Qian, "Resource Allocation for Multi-UAV Aided IoT NOMA Uplink Transmission Systems," *IEEE Internet Things J.*, vol. 6, no. 4, Aug. 2019.

[50] S. Zhang, J. Liu and W. Sun, "Stochastic Geometric Analysis of Multiple Unmanned Aerial Vehicle-Assisted Communications Over Internet of Things," *IEEE Internet Things J.*, vol. 6, no. 3, pp. 5446-5460, June 2019.